Chapter 15
Titanium and Titanium Alloy Applications in Medicine

M.J. Jackson, J. Kopac, M. Balazic, D. Bombac, M. Brojan and F. Kosel

Abstract Titanium is a transition metal. It is present in several minerals including rutile and ilmenite, which are well dispersed over the Earth's crust. Even though titanium is as strong as some steels, its density is only half of that of steel. Titanium is broadly used in a number of fields, including aerospace, power generation, automotive, chemical and petrochemical, sporting goods, dental and medical industries. The large variety of applications is due to its desirable properties, mainly the relative high strength combined with low density and enhanced corrosion resistance. This chapter discusses the applications of titanium and its alloys in the medical field.

15.1 Metallurgical Aspects

15.1.1 Introduction

Among the metallic materials, titanium and its alloys are considered the most suitable materials in medical applications because they satisfy the property requirements better than any other competing materials, such as stainless steels, Cr–Co alloys, commercially pure (CP) Nb and CP Ta [1–6]. In terms of biomedical applications, the properties of interest are biocompatibility, corrosion behavior, mechanical behavior, ability to be processed, and availability [7–9].

Titanium may be considered as being a relatively new engineering material. It was discovered much later than the other commonly used metals, its commercial application started in the late 1940s, mainly as structural material. Its usage as implant material began in the 1960s [10]. Despite the fact that titanium exhibits superior corrosion resistance and tissue acceptance when compared with stainless

M.J. Jackson (✉)
Kansas State University, Salina, KS, USA
e-mail: jacksonmj04@yahoo.com

J. Kopac · M. Balazic · D. Bombac · M. Brojan · F. Kosel
University of Ljubljana, Ljubljana, Slovenia

steels and Cr–Co-based alloys, its mechanical properties and tribological behavior restrain its use as biomaterial in some cases. This is particularly true when high mechanical strength is necessary, like in hard tissue replacement or under intensive wear use [11]. To overcome such restrictions, CP titanium was substituted by titanium alloys, particularly, the classic grade 5, i.e., Ti-6Al-4V alloy. The Ti-6Al-4V α + β-type alloy, the most worldwide utilized titanium alloy, was initially developed for aerospace applications [12, 13]. Although this type of alloy is considered a good material for surgically implanted parts, recent studies have found that vanadium may react with the tissue of the human body [2]. In addition, aluminum may be related with neurological disorders and Alzheimer's disease [2]. To overcome the potential vanadium toxicity, two new vanadium-free α + β-type alloys were developed in the 1980s. Vanadium, a β-stabilizer element, was replaced by niobium and iron, leading to Ti-6Al-7Nb and Ti-5Al-2.5Fe (α + β)-type alloys [4, 6, 14]. While both alloys show mechanical and metallurgical behavior comparable to those of Ti-6Al-4V, a disadvantage is that they all contain aluminum in their compositions.

In recent years, several studies have shown that the elastic behavior of α + β-type alloys is not fully suitable for orthopedic applications [15–18]. A number of studies suggest that unsatisfactory load transfer from the implant device to the neighboring bone may result in its degradation [9]. Also, numerical analyses of hip implants using finite element method indicate that the use of biomaterials with elastic behavior similar to cortical bones improves the distribution of stress around the implanted bone [19]. While the elastic modulus of a cortical bone is close to 18 GPa [7], the modulus of Ti-6Al-4V alloy is 110 GPa [7]. In such a case, the high elastic modulus of the implant material may lead to bone resorption and possible unsuccessful implantation procedure. The elastic behavior mismatch between the implant and the adjacent bone is named the 'stress shielding effect' [19].

Since CP titanium and some specific α + β-type titanium alloys do not completely meet the demands of medical applications, especially concerning mechanical behavior and toxicity to human body, a new class of alloys has been investigated for biomedical applications in the past decade, the β-type alloys. After proper heat treatments, these types of alloys may exhibit low elastic modulus, very good corrosion resistance, suitable mechanical properties after proper heat treatments, and good biocompatible behavior, as they may be obtained by adding biocompatible alloying elements like Nb, Ta, and Zr to titanium [20–24].

15.1.2 Basic Aspects of Titanium Metallurgy

The microstructure diversity of titanium alloys is a result of an allotropic phenomenon. Titanium undergoes an allotropic transformation at 882 °C. Below this temperature, it exhibits a hexagonal close-packed (HCP) crystal structure, known as α-phase, while at higher temperature it has a body-centered cubic (BCC) structure, β-phase. The latter remains stable up to the melting point at 1670 °C [5]. As
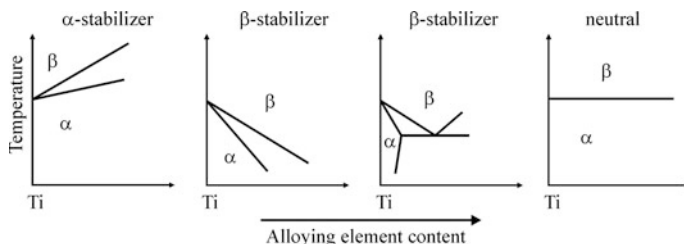
Fig. 15.1 Schematic representation of types of phase diagram between titanium and its alloying elements [5, 25]

titanium is a transition metal, with an incomplete d-shell, it may form solid solutions with a number of elements and hence, α- and β-phase equilibrium temperature may be modified by allowing titanium with interstitial and substitutional elements.
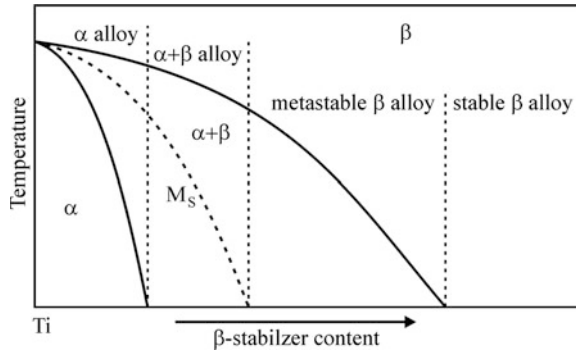
Titanium alloying elements fall into three class: α-stabilizers, β-stabilizers, and neutral. While elements defined as α-stabilizers lead to an increase in the allotropic transformation temperature, other elements, described as β-stabilizers provoke a decrease in such a temperature [25]. When a eutectoid transformation takes place, this β-stabilizer is termed eutectoid β-stabilizer, otherwise, it is called isomorphous β-stabilizer. If no significant change in the allotropic transformation temperature is observed, the alloying element is defined as neutral element. Figure 15.1 shows a schematic representation of types of phase diagram between titanium and its alloys elements [5, 25].

As a result, titanium alloys with an enormous diversity of compositions are possible. Among α-stabilizer elements are the metals of IIIA and IVA groups (Al and Ga) and the interstitials C, N, and O. On the contrary, β-stabilizer elements include the transition elements (V, Ta, Nb, Mo, Mg, Cu, Cr, and Fe) and the noble metals.

Addition of α- and β-stabilizer elements to titanium gives rise to a field in the corresponding phase diagram where both α- and β-phase may coexist. Titanium alloys exhibit a variety of properties, which are connected to chemical composition and metallurgical processing [26–28]. According to the nature of their microstructure, titanium alloys may be divided as either α-alloys, β-alloys, and α + β-alloys [29]. Beta alloys may be further classified into near β and metastable β-alloys.

Alpha titanium alloys are especially formed by CP titanium and alloys with α-stabilizer elements, which present only α-phase at room temperature. Such alloys show high creep resistance and are thus suitable for high temperature service. Since no metastable phase remains after cooling from high temperature, no major modification in terms of microstructure and mechanical properties are possible using heat treatments. Finally, as α-phase is not subjected to ductile–brittle transition, these alloys are proper for very low temperature applications. Regarding mechanical and metallurgical properties, α-alloys present a reasonable level of mechanical strength, high elastic modulus, good fracture toughness, and low plastic deformation, which is due to the HCP crystal structure.

Fig. 15.2 Partial phase diagram of titanium and a β-stabilizer element [5, 6]
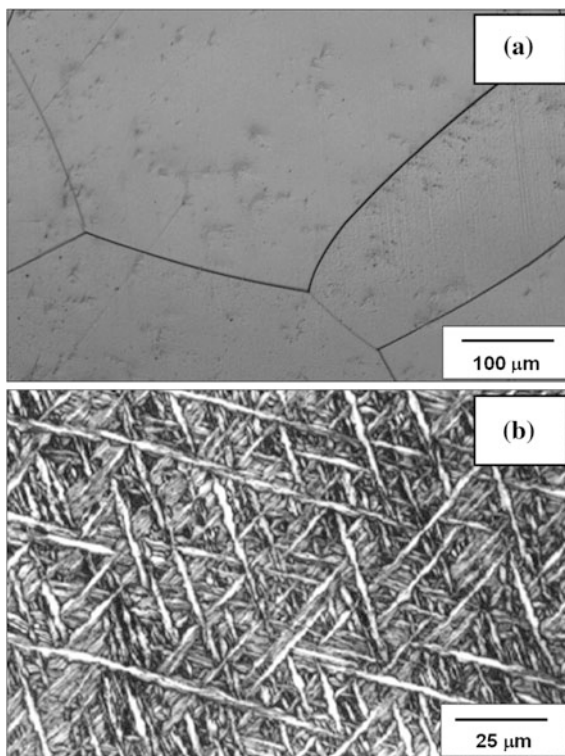
Beta titanium alloys are obtained when a high amount of β-stabilizer elements are added to titanium, which decreases the temperature of the allotropic transformation (α/β transition) of titanium [30]. If the β-stabilizer content is high enough to reduce the martensitic start temperature (M_S) to temperatures below the room temperature, nucleation and growth of α-phase will be very restricted, and hence, metastable β is retained at room temperature under rapid cooling, as depicted in Fig. 15.2. This type of titanium alloy may be hardened using heat treatment procedures [31]. In some cases, depending upon composition and heat treatment parameters, precipitation of ω-phase is possible. However, ω-phase may cause embrittlement of a titanium alloy and, in general its precipitation must be avoided [32]. β-titanium alloys are very brittle at cryogenic temperatures and are not meant to be applied at high temperatures, as they show low creep resistance.

Finally, α + β-*alloys* include alloys with enough α- and β-stabilizers to expand the α + β field to room temperature [5, 25]. The (α and β) phase combination allows one to obtain an optimum balance of properties. The characteristics of both α- and β-phases may be tailored by applying proper heat treatments and thermo-mechanical processing. A significant assortment of microstructures may be obtained when compared to α-type alloys. The Ti-6Al-4V alloy is an example of α + β-type alloy. Due to its large availability, very good workability, and enhanced mechanical behavior at low temperatures, such an alloy is the most common composition among the titanium alloys and based on these characteristics it is still largely applied as a biomaterial, mainly in orthopedic implant devices. Figure 15.3 depicts the microstructures of β and α + β-titanium alloys.

As in the case of iron (steels), allotropic transformation is the main reason for the enormous variety of microstructure in titanium alloys. Titanium alloy microstructures are formed by stable and metastable phases [33, 34]. In general, for limited β-stabilizer content and depending on cooling conditions, titanium alloys show only α- and β-phases.

However, if the thermodynamic equilibrium is not reached, metastable phases may be retained at room temperature, mainly, martensitic and ω-phases. According to several authors [35–37], titanium alloys with β-stabilizer elements such as Mo, Nb, Ta, and V, may form two types of martensitic structures. If the β-stabilizer

Fig. 15.3 Microstructures of
a β Ti-35Nb (wt%) and
b α + β Ti-6Al-7Nb (wt%)
alloys cooled in air

content is considered low, rapid cooling leads to formation of hexagonal martensite, termed α′. When this content is high α′ martensite undergoes a distortion, loses its symmetry, and is substituted by orthorhombic martensite, defined as α″ [37].
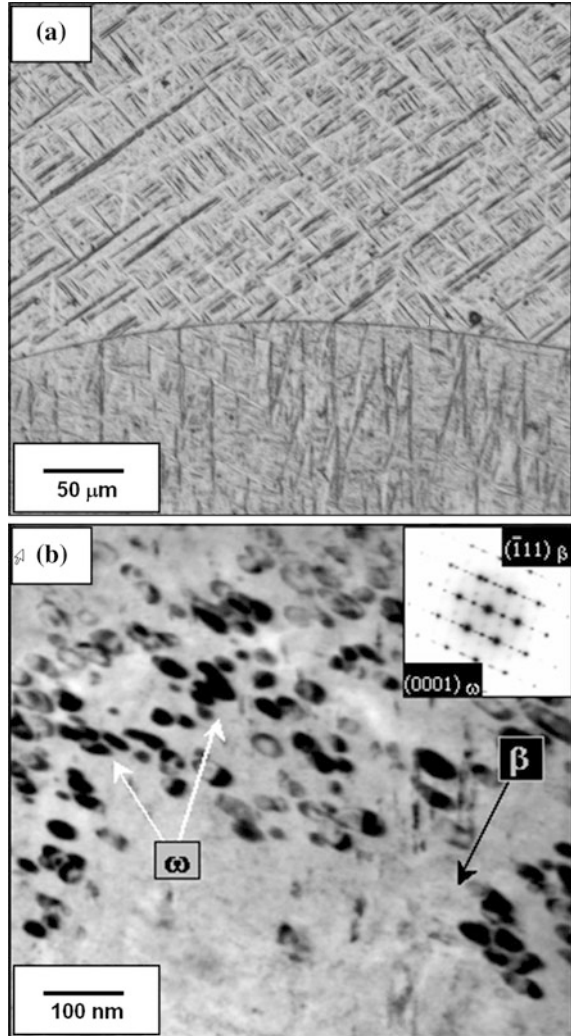
When titanium alloys with β-stabilizer elements are submitted to rapid cooling from high temperature, the β-phase may transform either in martensitic structures or eventually, in metastable ω-phase [35]. Figure 15.4 presents a microstructure of the Ti-25Nb (wt%) after cooling in water and in air showing α″ and ω formation.

Precipitation of ω-phase occurs only in a limited range of the alloy element and may arise during the quenching from high temperature (β-phase), forming a thermal ω-phase. However, ω-phase may also form after aging of a rapid by quenched structure at medium temperatures, resulting in isothermal ω-phase, as indicated in Fig. 15.5.

15.1.3   Mechanical Behavior

Concerning mechanical behavior, biomedical titanium alloys applied as biomaterial mainly in hard tissue replacement, must exhibit a low elastic modulus combined

Fig. 15.4 Microstructure of the Ti-25Nb (wt%) alloy: **a** water cooled sample showing martensitic structure (MO analysis) and **b** air cooled sample showing ω phase dispersed in β matrix and respective SADP showing ω and β phases microstructure (TEM analysis)

with enhanced strength, good fatigue resistance, and good workability. Mechanical behavior of titanium alloys is directly related to composition and mainly, thermo-mechanical processing. Some mechanical properties of selected titanium-based materials applied as biomaterials are shown in Table 15.1 [38].

Mechanical strength may be increased by adding alloying elements, which may lead to solid-solution strengthening or even, precipitation of second phases. Also, using aging processes, metastable structures obtained by rapid quenching from β field may give rise to fine precipitates, which considerably increases mechanical strength.

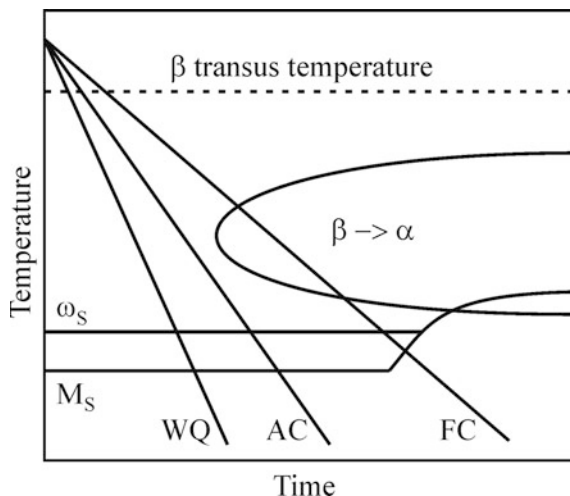Fig. 15.5 A schematic TTT diagram for β phase transformation in titanium alloys with β-stabilizer elements [35]

Table 15.1 Selected Ti-based materials developed for medical applications [38]

Material	Tensile strength (MPa)	Yield strength (MPa)	Elongation (%)	Elastic modulus (GPa)
α type				
Pure Ti grade 1	240	170	24	102.7
Pure Ti grade 2	345	275	20	102.7
Pure Ti grade 3	450	380	18	103.4
Pure Ti grade 4	550	485	15	104.1
α + β type				
Ti-6Al-4V	895–930	825–869	6–10	110–114
Ti-6Al-4V ELI	860–965	795–875	10–15	101–110
Ti-6Al-7Nb	900–1050	880–950	8.1–15	114
Ti-5Al-2.5Fe	1020	895	15	112
β type				
Ti-13Nb-13Zr	973–1037	836–908	10–16	79–84
Ti-12Mo-6Zr-2Fe	1060–1100	1000–1060	18–22	74–85
Ti-15Mo	874	544	21	78
Ti-15Mo-5Zr-3Al	852–1100	838–1060	18–25	80
Ti-15Mo-2.8Nb-0.2Si	979–999	945–987	16–18	83
Ti-35.3Nb-5.1Ta-7.1Zr	596.7	547.1	19	55
Ti-29Nb-13Ta-4.6Zr	911	864	13.2	80

Titanium alloys present a high strength-to-weight ratio, which is higher than with most of steels. While CP titanium has yield strength between 170 (grade 1) and 485 MPa (grade 4), titanium alloys may present values higher than 1500 MPa [25].

The elastic modulus or Young modulus corresponds to the stiffness of a material and is associated to the way inter-atomic forces vary with distance between atoms in the crystal structure. A comparison between both crystal structures of titanium has led to the conclusion that HCP structure presents higher values of elastic modulus than the BCC structure. Hence, addition of β-stabilizer elements allows β-phase stabilization and hence, low elastic modulus alloys. While CP titanium shows elastic modulus values close to 105 GPa, Ti-6Al-4V-type α + β alloy presents values between 101 and 110 GPa, type-β titanium alloys may present values as low as 55 GPa [38]. When compared with common alloys used as biomaterials, such 316 L stainless steel (190 GPa) and Co–Cr alloys (210–253), low elastic modulus titanium alloys display a more compatible elastic behavior to that of the human bone [39]. In general, as the elastic modulus decreases, so does the mechanical strength and vice versa.

Analysis of slip systems in different crystal structures reveals that plastic deformation is easier in BCC crystal structure than in HCP structure. It explains the enhanced ductility of β-phase when compared to α-phase. In a HCP structure, the number of slip systems is only three, while this number increases to 12 in the case of BCC structure. In addition, the ease of plastic deformation facility is directly connected to the minimum slip distance, b_{min} [25], which is given by the inter-atomic distance divided by the respective lattice parameter. Since, HCP structure exhibits a higher slip distance than BCC structure, it is possible to conclude that the atomic planes slip or the plastic deformation is easier in BCC structure than HCP. Hence, β-type alloys present the best formability among the titanium alloys.
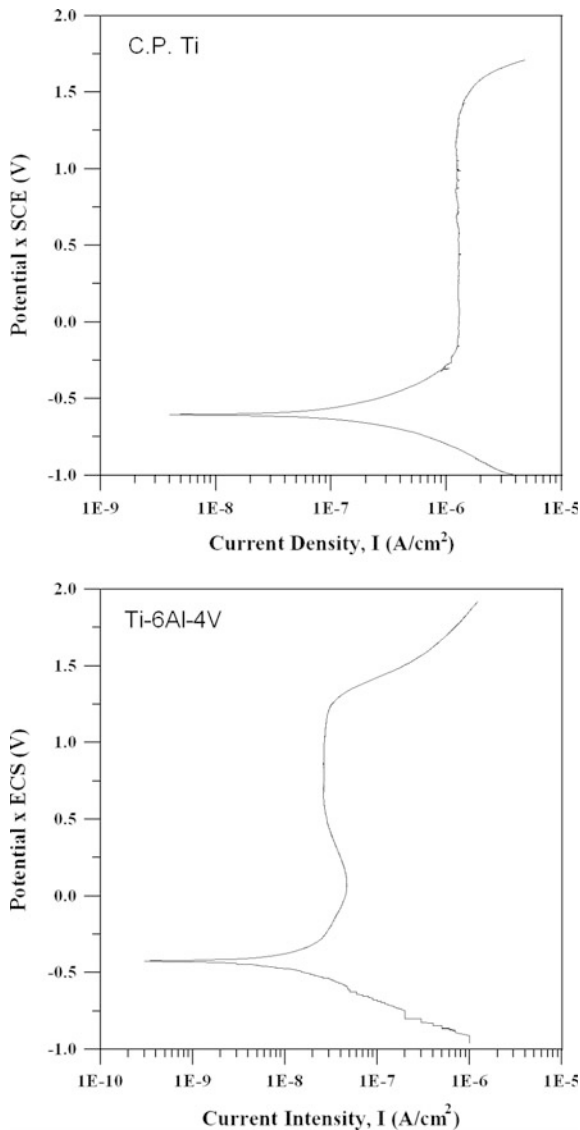
15.1.4 Corrosion Behavior

Corrosion resistance is one of the main properties of a metallic material applied in the human body environment and the success of an implant depends on the careful examination of this phenomenon. The performance of an implant is directly related to its ability in functioning in the aggressive body fluids. In general, these fluids consist of a series of acids and certain amount of NaCl. In normal conditions, its pH is 7, however, it may be altered due to immune system response, like in the case of an infection or inflammation. In an event of a corrosion process, the implant component may lose its integrity, leading to a failure. In addition, release of corrosion products may lead to undesirable biological reactions. Certainly, this will depend on the nature of chemical reactions on the implant surface in view of the fact that corrosion is essentially a chemical process.

Titanium shows an excellent corrosion resistance, which is directly related to the formation of a stable and protective oxide layer, essentially TiO_2. The reactivity of titanium can be measured by its standard electrode potential (standard electromotive force (EMF) series), which is −1.63 V [5]. Such a value indicates that titanium has a high chemical reactivity and is easily oxidized, giving rise to a very adherent and

thin oxide layer on the titanium surface. This oxide layer passivates the titanium, which results in a protection against further corrosion process as long as this layer is maintained. Actually, formation of passivation films on titanium does not mean cessation of corrosion processes. It means that the corrosion rate will be significantly reduced. Therefore, titanium is corrosion resistant in oxidizing environments but not resistant in reducing medium [5].

In general, anodic polarization testing is an efficient method of analyzing corrosion behavior of metallic material in a corrosive environment. Figure 15.6 depicts

Fig. 15.6 Polarization curves for CP titanium and Ti-6Al-4V alloy (Scan rate of 0.1 mV s^{-1})

the anodic polarization curve for CP titanium and Ti-6Al-4V alloys, showing the electric current intensity versus potential (versus saturated calomel electrode (SCE)), obtained with 5 g/l NaCl, pH 4 solution as an electrolytic medium at 310 K. The potential was scanned at 0.1 mV s^{-1} [11].

The anodic portion of the polarization curve allows one to evaluate the corrosion behavior of a metallic material in an electrolytic medium. Evaluation is obtained by determining the range of potentials in which passivation films are stable, and also by finding the current intensity of passivation. As usual, polarization tests started at a negative potential of −1.0 V versus SCE, reaching more positive values. In such a process, the initial sector of the anodic polarization curve refers to the beginning of a corrosion phenomenon, where the metallic material reacts with the supporting electrolyte, leading to active corrosion.

The following segment is related to the formation of an oxide passivation film, when the electric current stabilization takes place. As the potential increases, the current intensity also increases and eventually, the rupture of passivation film occurs. At this point, the protective layer loses its efficiency causing pitting corrosion. However, this hypothesis is not confirmed during the reverse scanning of potential. Polarization curves obtained during forward and backward scans of potential are superimposed and no pitting potential is observed, which allows one to conclude that both materials show outstanding resistance to corrosion.

15.2 Principal Requirements of Medical Implants

15.2.1 Introduction

Medical implants are products that have to satisfy the functionality demands defined by the working environment-human body. They could be used in almost every organ of the human body. Ideally, they should have biomechanical properties comparable to those of autogenous tissues without any adverse effects. The principal requirements of all medical implants are corrosion resistance, biocompatibility, bioadhesion, biofunctionality, processability, and availability. To fulfill these requirements most of the tests are directed into the study extracts from the material, offering screens for genotoxicity, carcinogenicity, reproductive toxicity, cytotoxicity, irritation, sensitivity, and sterilization agent residues [40]. The consequences of corrosion are the disintegration of the implant material per se, which weakens the implant, and the harmful effect of corrosion on the surrounding tissues and organs is produced.

Medical implants are regulated and classified in order to ensure safety and effectiveness to the patient. One of the main goals of implant research and development is to predict long-term, in vivo performance of implants. Lack of useful computer-modeling data about in vivo performance characteristics makes the evaluation of synergistic contributions of materials, design features, and therapeutic drug regimens difficult. The present trends in modern implant surgery are

networking various skilled and gifted specialists such as trauma specialists, orthopedists, mechanical engineers, pharmacists, and others in order to get better results in research, development and implementation into practice.

15.2.2   Metallic Biomaterials

The first metal alloy developed specifically for the human body environment was the 'vanadium steel' that was used to manufacture bone fracture plates (Sherman plates) and screws. Most metals that are used to make alloys for manufacturing implants such as iron (Fe), chromium (Cr), cobalt (Co), nickel (Ni), titanium (Ti), tantalum (Ta), niobium (Nb), molybdenum (Mo), and tungsten (W), can only be tolerated by the body in minute amounts. Sometimes these metallic elements, in naturally occurring forms, are essential in red blood cell functions (Fe) or synthesis of a vitamin B_{12} (Co), etc. but cannot be tolerated in large amounts in the body [41].
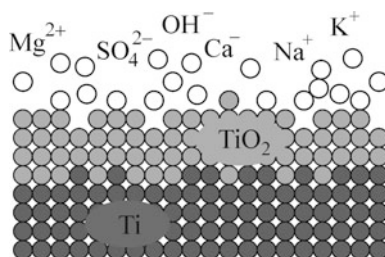
Metallic biomaterials can be divided into four subgroups: stainless steels, the cobalt-based alloys, titanium metals, and miscellaneous others (including tantalum, gold, dental amalgams, and other special metals). They are very effective in binding the fractured bone, do not corrode, and do not release harmful toxins when exposed to body fluids and therefore can be left inside the body for a long period of time. Their disadvantage is a much larger hardness and stiffness compared to the bone and possibility of interfering with the regrowth of the bone.

15.2.3   The Surface-Tissue Interaction

Good corrosion resistance of titanium depends upon the formation of a solid oxide layer (TiO_2) to a depth of 10 nm. After the implant is inserted, it immediately reacts with body liquids that consist of water molecules, dissolved ions, and proteins as shown in Fig. 15.7.

Geometry, roughness, and other characteristics of the implant surface also importantly influence the surface-tissue interaction, which is considered to be dynamic. Due to these phenomena, over time new stages of biochemical formations

Fig. 15.7 Interaction between titanium and body liquids [129]

can be developed. In the first few seconds, after the contact has been made, there is only water, dissolved ions, and free biomolecules in the closest proximity of the surface, but no cells. The composition of the body liquid changes continuously as inflammatory and healing processes continue to proceed, causing changes in the composition of the adsorbed layer of biomolecules on the implant surface until it is balanced. Cells and tissues eventually contact the surface and, depending on the nature of the adsorbed layer, they respond in specific ways that may further modify the adsorbed biomolecules [42].

Surface roughness also plays an important role in osteointegration. Osteoblast cells are more likely to get attached to rough-sand blasted surfaces, meaning lower cell numbers on the rougher surfaces, decreased rate of cellular proliferation, and increased matrix production compared to smooth surface. Experiments made by Feighan [43] showed that an average roughness increased from 0.5 to 5.9 μm also increase the interfacial shear strength from 0.48 to 3.5 MPa.

15.2.4 Machining of Titanium Alloys

Titanium alloys are among the most widely used and promising materials for medical implants. Selection of titanium alloy for implementation is determined by a combination of the most desirable characteristics including immunity to corrosion, biocompatibility, shear strength, density, and osteointegration [3]. The excellent chemical and corrosion resistance of titanium is to a large extent due to the chemical stability of its solid oxide surface layer to a depth of 10 nm [44]. Under in vivo conditions, the titanium oxide (TiO_2) is the only stable reaction product whose surface acts as catalyst for a number of chemical reactions. However, micromotion at the cement-prosthesis and cement-bone are inevitable and consequently, titanium oxide and titanium alloy particles are released in the cemented joint prosthesis. Sometimes this wear debris accumulates as periprosthetic fluid collections and triggers giant cell response around the implants [45]. TiO_2 film, such as the ones anodically formed in aqueous electrolytes, consists mainly of anatase and is an n-type semiconductor with low electronic charge conductivity and a high resistance to anodic current [46].

Processes of machining titanium alloys involve conventional machining operations (turning, face milling, high-speed cutting (HSC), milling, drilling), forming operations (cold and hot forming; hydroforming, forging) and alternative machining operations (laser cutting, waterjet cutting, direct metal laser sintering). Machining operations of titanium alloys are considered to be difficult, due to its relatively high tensile strength, low ductile yield, 50 % lower modulus of elasticity (104 GPa) and approximately 80 % lower thermal conductivity than that of steel [47]. The lower modulus of elasticity may cause greater 'spring back' and deflection effect of the workpiece. Therefore, more rigid setups and greater clearances for tools are required. In the tool contact zones high pressures and temperatures occur (the tool-to-workpiece interface). The amount of heat removed by laminar chips is only

approximately 25 %, the rest is removed via the tool. Due to this phenomenon titanium alloys can be machined at comparatively low cutting speeds. At higher temperatures caused by friction the titanium becomes more chemically reactive and there is a tendency for titanium to » weld « to tool bits during machining operations. Over-heating of the surface can result in interstitial pickup of oxygen and nitrogen, which will produce a hard and brittle alpha case. Carbides with high WC–Co content (K-grades) and high-speed steels with high cobalt content are suitable for use as cutting materials in titanium machining operations [47]. Turning operations of titanium alloys should have cutting depths as large as possible, cutting speeds V_C from 12 to 80 m/min and approximately 50 % lower when high-speed steel (HSS) tools are used. The heat generated should be removed via large volumes of cooling lubricant. Chlorinated cutting fluids are not recommended because titanium can be susceptible to stress corrosion failures in the presence of chlorine. Any type of hot working or forging operation should be carried out below 925 °C due to the high level of titanium reactivity at high temperature.

Some medical implants are produced modularly, using different materials and processing techniques. For example, the femoral stem as part of the hip endoprosthesis is produced in a combination of casting, forging, and milling. The final machining operation is performed on CNC machine using CAD-CAM principle.

Good alternatives to conventional machining techniques are alternative techniques such as waterjet cutting, sintering, or direct metal laser sintering. The latter is a rapid prototyping technique enabling prompt modeling of metal parts with high bulk density on the basis of individual three-dimensional data, including computer tomography models of anatomical structures. The concept of layer by layer building rather than removing waste material to achieve the desired geometry of a component opens up endless possibilities of alternative manufacture of medical devices and is more environment friendly.

Even though machining Ti alloys produces forces only slightly higher than those developed when machining steel, the specific metallurgical characteristics of these alloys create difficulties and therefore increase the price. Although hard, it is not impossible to achieve excellent surface finish and good production rates when these alloys are machined, however, it is necessary to take into consideration the very unique characteristics which Ti alloys posses such as low heat conduction, reactivity, low Young's modulus, alloying tendency, surface damage susceptibility, and work hardening characteristics. The following review of machining titanium and its alloys are shown in greater detail in reference [48].

Poor heat conduction of Ti alloys makes the heat linger on the tool cutting edge and tool face effecting tool life. Furthermore the work hardening characteristics of the alloy induces the absence of a built-up edge creating localization of heat that in combination with high bearing forces results in rapid tool deterioration. The spring back effect in these alloys is high due to the low Young's modulus and consequently the deflections of the workpiece are significant making precision machining hard. Increasing the systems rigidity, using sharp tools, greater tool clearances are one of the ways to reduce this effect. Surface damage in Ti alloys has an effect when they are used in application where fatigue life is important. In the aim of optimizing

fatigue life it is necessary to maintain sharpness of the tools while machining (mostly grinding) titanium alloys. Main influencing parameters when machining Ti alloys to be considered are as follows:

– Cutting speed
– Feed rate
– Cutting fluid
– Tool sharpness
– Tool–workpiece contact
– Rigidity of the setup.

When setting up the machining parameters for machining Ti alloys, it is necessary to keep the speed low in order to minimize the temperature rise and consequently reduce the influence of heat on the tool tip and edge. Since the tool temperature is affected more by speed and less by feed, than the feed should be kept high while taking into consideration that a work hardened layer is formed after each cut and the consecutive cut needs to be larger than the thickness of this layer. Another influence on the temperature during machining is the amount of cutting fluid used. A generous amount needs to be used to reduce temperatures as well as to clear the work area of chips and reduce cutting forces. The sharpness of the tools used in machining is going to influence the surface finish and if not adequate can cause tearing as well as deflection of the workpiece. The contact of the tool with the workpiece is important due to the fact that if dwelling of the tool is allowed while tool is in contact with the workpiece it can cause work hardening, smearing, galling, and seizing leading to tool deterioration and eventually breakdown. Most of the efforts made to enhance the machining process of titanium alloys have been focused on decreasing temperature generated at the cutting edge and tool face due to the fact that it influences tool life and surface characteristics of the workpiece. It has been shown that when machining Ti6Al4V alloys, tool life is increased by decreasing cutting speed and increasing feed. At high cutting speeds, the tool deteriorates rapidly and tool life is dramatically increased by lowering the speed parameter [49].

The cutting tool material needs to offer abrasion resistance and hot hardness and so far the three most satisfying materials have been proven to be carbide and high speed or highly alloyed steels. Different materials are used for different applications, for example, turning and face milling is mostly done using C2 tungsten carbide grades while HSS tools are used for milling, drilling, and tapping of Ti alloys. Productivity is also being influenced using specific techniques such as specially designed cutters and special cutting techniques [49].

Milling parameter recommendations are given in Tables 15.2, 15.3, and 15.4, for face milling, end milling–slotting, and end milling–peripheral milling, consecutively. The change in cutting speed and/or feed has a significant influence on the chip–tool contact length, chip length, segmentation frequency, segment size, and chip thickness therefore presents the two major parameters for process manipulation. Owing to this fact, the effect of machining parameters such as cutting speed and feed on chip formation has been a topic of interest for many researchers [49].

Table 15.2 Face milling data [49]

Material	Condition	Doc, in	HSS tool			Carbide tool		
			Speed, fpm	Feed in/tooth	Tool material	Speed, fpm	Feed in/tooth	Tool material
Ti6Al4V	Annealed	0.25	40	0.006	M3/T15	130	0.006	C2
Ti6Al4V ELI	Annealed	0.05	50	0.004	M3/T15	170	0.004	C2

It has been shown that there is a dependence of the contact length on the cutting speed when machining Ti6Al4V alloys where the contact length is considered to be the contact between the chip and the tool rake face when creating a continuous chip [50]. The dependence presented in Fig. 15.8 shows that there is a maximum contact length that is achieved at the transition in the cutting speed from regular to high speed. They attribute this dependence to the effect of "shear banding." The contact length is also shown to be dependent on the undeformed chip thickness, where the increase in the undeformed chip thickness yields an increase in the contact length. It has been stated that the chip compression ratio (ratio of the actual and undeformed hip thickness) is hard to comprehend due to the scattered results and they attribute this to the poor machinability of Ti alloys and shear banding as well.

Chip morphology has been researched [51] showing that the saw-chip formation is present and that the chip length is increased while the width decreased with the increase in cutting speed and feed. The segmentation size increases while the frequency of the segmentation decreases with cutting speed. This has also been determined in further work [52], where it has been shown that the segmentation frequency increases linearly with the increase in cutting speed and decreases with increase in feed (Fig. 15.9).

The chip thickness ratio (ratio of undeformed chip thickness and actual chip thickness) has been shown to increase with the decrease in cutting speed and it decreases with the increase in feed when using low speeds (Fig. 15.10) [53].

The dependence of chip thickness, tool–chip contact length and chip up-curl radius on the tool radius/chip thickness ratio has been presented in Fig. 15.11 [54]. The chip thickness decreases with the increase in the tool radius value as the ratio of the tool radius and undeformed chip thickness is increased. The tool–chip contact length follows the same trend as the chip thickness yielding a lower value with the increase of the tool edge radius.

However, the chip thickness is a questionable parameter when Ti alloys are being investigated [55]. The conventional chip thickness ratio for the continuous chip formation models and the parameters such as shear angle which are calculated from the ratio are considered to be incorrect parameters for describing machining characteristics of Ti alloys [55]. This is due to the fact that Ti alloy chips become deformed inconsequentially, and are formed by gradual flattening of a softer half wedge by the tool. Consequently, the chip thickness ratio is close to unity. This is one of the reasons that when machining Ti alloys, the shear angle cannot be assessed using a conventional formula as it can when machining steel where

Table 15.3 End milling data—slotting [49]

Material	Condition	Doc, in	High-speed tool (M2)					Carbide tool (C2)				
			Speed, fpm	Cutter diameter, in				Speed, fpm	Cutter diameter, in			
				Feed per tooth					Feed per tooth			
				1/18	3/8	3/4	1–2		1/8	3/8	3/4	1–2
Ti6Al4V	Annealed	0.25	30	–	0.0007	0.003	0.004	75	–	0.0007	0.003	0.005
Ti6Al4V	Annealed	0.125	40	–	0.001	0.003	0.004	100	–	0.0015	0.003	0.005
ELI		0.050	50	0.0005	0.002	0.004	0.005	125	0.0005	0.002	0.005	0.007
		0.015	65	0.0007	0.003	0.005	0.006	165	0.0005	0.003	0.006	0.008

Table 15.4 End milling data—peripheral milling [49]

Material	Condition	Doc, in	High-speed tool (M2)					Carbide tool (C2)				
			Speed, fpm	Cutter diameter, in				Speed, fpm	Cutter diameter, in			
				Feed per tooth					Feed per tooth			
				1/8	3/8	3/4	1–2		1/8	3/8	3/4	1–2
Ti6Al4V	Annealed	0.25	50	–	0.001	0.004	0.005	125	–	0.001	0.004	0.006
Ti6Al4V ELI	Annealed	0.125	60	–	0.0015	0.004	0.005	150	–	0.002	0.004	0.006
		0.050	75	0.0008	0.003	0.005	0.006	190	0.0008	0.003	0.006	0.007
		0.015	90	0.001	0.004	0.006	0.007	225	0.001	0.004	0.007	0.008

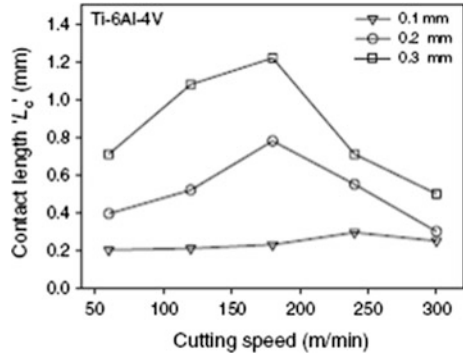**Fig. 15.8** Variation of the contact length with cutting speed for Ti6Al4V [50]

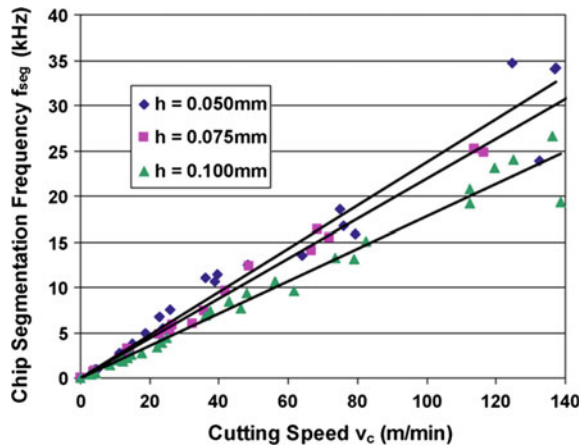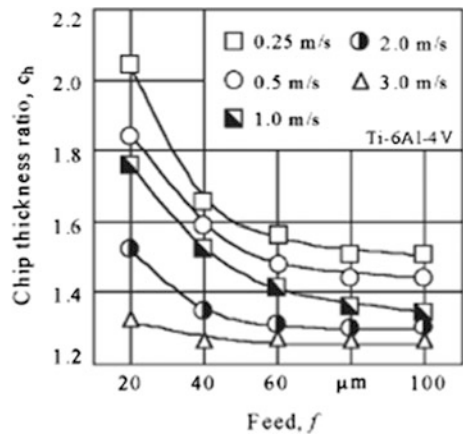**Fig. 15.9** Dependence of chip segmentation frequency on cutting speed [51]

Fig. 15.10 Chip thickness ratio as a function of cutting speed and feed for Ti6Al4V [53]
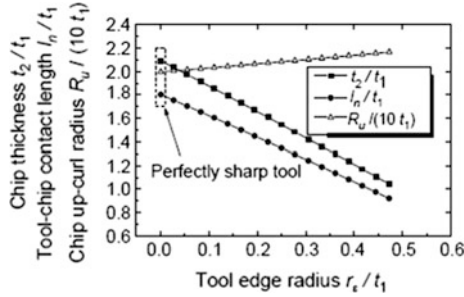
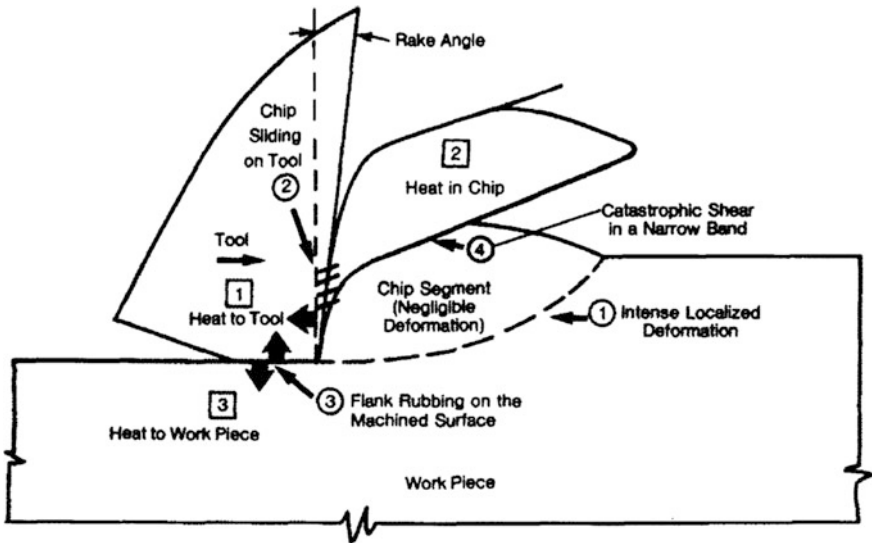**Fig. 15.11** Influence of the tool edge radius [54]

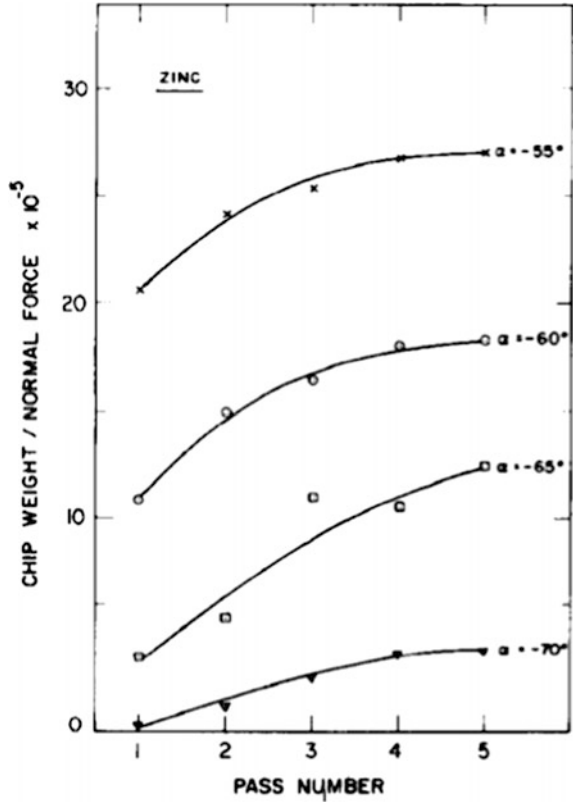**Fig. 15.12** Energy partition when machining Ti alloys [55]

concentrated shear subjects the chip to large strain creating thick chips with low shear angles and low velocity. Energy partition presented in Fig. 15.12 is also different from steel showing:

– Energy into the chip $U_c = R_1 U_s$
– Into the tool $U_t = (1 - R_1)U_s + R_3 U_{ff}$
– Into the workpiece $U_w = (1 - R_3)U_{ff}$.

(U_{ff} is the frictional energy per unit volume due to rubbing between the flank and the machined surface and R_3 is the fraction of heat conducted into the tool due to flank friction).

The high temperatures are present when using low values of the depth of undeformed layers due to the rubbing of the flank on the machined surface. When

Fig. 15.13 Influence of the rake angle on chip formation [56]

the influence of the rake angle on the chip formation [56] has been investigated, it has been determined that the rake angle has a critical value of −70° when machining zinc, after which there is no chip formation (Fig. 15.13).

This issue has further been addressed [57] where it has been determined that the rake angle at which chip formation seizes is −85°. While elsewhere [58] it has been determined that this value is lower and equals −55°. The mechanism of chip formation when machining Ti6Al4V alloys has been discussed by many researchers and follows two theories. The first theory is the catastrophic thermoplastic shear where thermal softening present in the primary shear zone predominates the strain hardening caused by high strain rates in machining. The second theory is the periodic crack initiation that is considered as a consequence of high stress present during the machining process. This theory is based on the idea that cracks are formed in the primary shear zone and then rewelded through high pressure and heat originating from friction. In the following paper [59], the authors show the formation of the chip and its microstructure showing the lack of cracks in Fig. 15.14. The authors have determined that there is no phase transformation taking place classifying the bands to be deformation shear bands and confirming the catastrophic shear model.
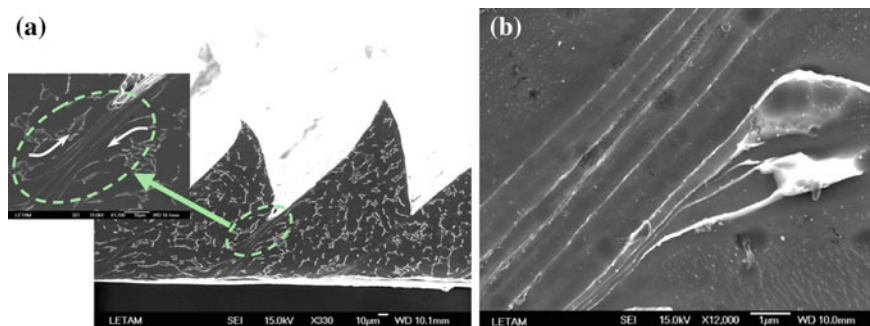
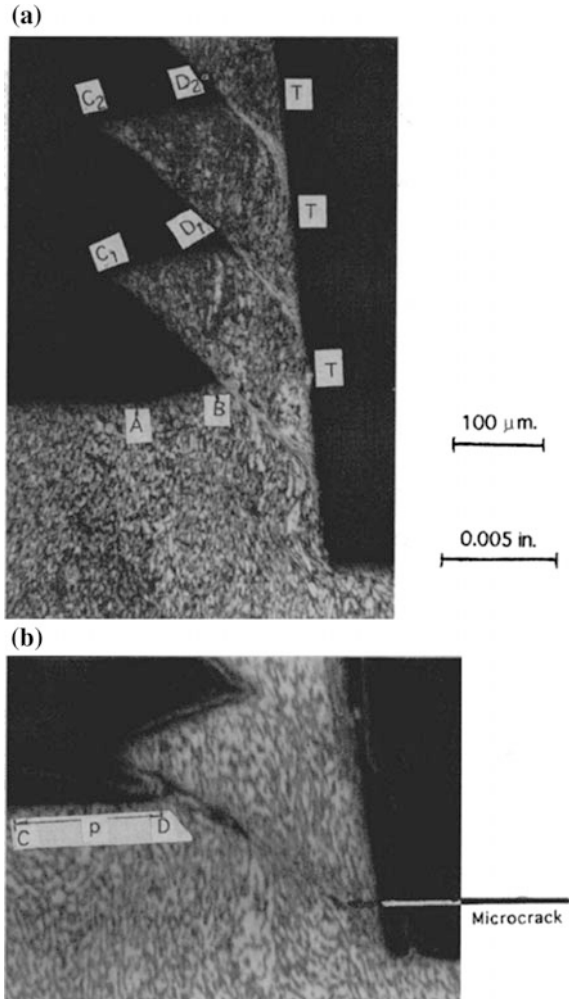**Fig. 15.14** Microstructure of the chips and shear bands in Ti6Al4V [59]

Vyas and Shaw on the other hand confirm the crack initiation presented in Fig. 15.15. They show formation of both gross cracks and micro cracks. Gross cracks continue throughout the chip width while micro cracks seem to be discontinuous. The process is based on the idea that the blocks of material which are between the gross cracks glide out with no plastic deformation while the material surrounding the micro cracks will undergo adiabatic shear in case that the temperature is high enough which may also result in phase transformations [60]. It is obvious from the fact that both theories are present and confirmed in the literature that the chip formation mechanism is not straightforward and must depend on various parameters. Investigation techniques such as X-ray diffraction, energy dispersive X-ray analysis, scanning electron microscopy, electron backscattering technique can be found useful in determining the causes of the discussed results. It is yet to be determined why these inconsistencies occur and what influences which one of the theories will be observed in the experimental work. Therefore, this can be considered a field with a vast potential for research.

15.2.5 Surface Treatments and Coatings

Mechanical methods for surface treatment can be divided into methods involving removal of surface material by cutting (machining of the surface), abrasive action (grinding and polishing) and those where the treated material surface is deformed by particle blasting. Chemical methods are based mainly on chemical reactions occurring at the interface between titanium and a solution (solvent cleaning, wet chemical etching, passivation treatments, and other chemical surface treatments such as hydrogen peroxide treatment). Electrochemical surface methods are based on different chemical reactions occurring at an electrically energized surface (electrode) placed in an electrolyte (electropolishing and anodic oxidation or anodizing).

Improving the method for both wear and corrosion resistance of titanium implant surfaces in cases where the protection by natural surface oxide films is insufficient

Fig. 15.15 Mechanics of chip formation showing **a** crack formation, **b** micro crack formation in Ti6Al4V [60]

(a)

100 μm.

0.005 in.

(b)

Microcrack

can be done through the deposition of thin films. These coatings should have a sufficiently high adherence to the substrate throughout the range of conditions to which the implant is exposed in service. They must tolerate the stress and strain variations that any particular part of the implant normally impose on the coating. The coating process must not damage the substrate and must not induce failure in the substrate or introduce impurities on the surface, which may change interface properties [46]. Coatings should be wear resistant, barrier layers preventive of substrate metal ion release, to low-friction haemocompatible, non-thrombogenic surfaces [46]. Such surface modification could be done by various processes such as precipitations from the chemical vapor phase, sol–gel coatings, chemical vapor deposition (CVD), or physical vapor deposition (PVD). The properties of PVD coatings are good thickness, roughness, hardness, strength, and adhesion as well as

structure, morphology, stoichiometry, and internal stresses. PVD processes include evaporation, sputtering, ion plating, and ion implantation. They are carried out in vacuum, at backpressures of less than 1 Pa [46]. Speaking of the CVD methods, they involve the reaction of volatile components at the substrate surface to form a solid product. Typical CVD coatings are depositions of TiN, TiC, and TiC_xN_{1-x}. The early coatings were deposited onto hard metal tools such as WC–Co. Good coating uniformity is an advantage of the CVD method, lower operating temperatures of PVD method that can be combined in the plasma-assisted CVD process. Biomaterial produced by low temperature CVD and PVD is diamond-like carbon (DLC). DLC coatings can address the main biomechanical problems with the implants currently used, e.g., friction, corrosion, and biocompatibility [61].

The concept of bioactive coatings uses a principle of enabling an interfacial chemical bond between the implant and the bone tissue due to a specific biological response [62]. Surface modifications should provide distinct properties of interaction with cell molecules, which promote the adaptation or in-growth of cells or tissue onto the surface of fixation elements of a medical implant or prevent cell interaction with the implant surface.

Suitable bioactive surface modifications are comparable to those known from the stoichiometrically passivated titanium surface, in terms of high mechanical stability against shearing forces, long-term chemical stability, and corrosion resistance in a biocompatible manner. One of the most popular bioactive coatings is hydroxyapatite (HA), which is similar to the mineral phase of natural hard tissue, i.e., about 70 % of the mineral fraction of a bone has a HA-like structure. HA can also be regarded as non-resorbable in a physiological environment, as long as it remains crystalline and is of high purity. It is the most stable calcium phosphate phase in aqueous solutions [63]. It has weaker mechanical properties and low resistance to fatigue failure. Surface treatments techniques for HA are plasma spraying (vacuum plasma spraying-VPS) electrophoretic deposition of HA and micro-arc oxidation.

15.2.6   Applications in Practice

Different types of fracture repair mechanisms are known in medical practice. Incomplete fractures such as cracks, which only allow micromotion between the fracture fragments, heal with a small amount of fracture-line callus, known as primary healing. In contrast, complete fractures that are unstable, and therefore generate macromotion, heal with a voluminous callus stemming from the sides of the bone, known as secondary healing. The treatments can be nonsurgical or surgical. Nonsurgical treatments are immobilization with plaster or resin casting and bracing with a plastic apparatus. The surgical treatments of bone fractures (osteosynthesis) are divided into external fracture fixation, which does not require opening the fracture site, or internal fracture fixation, which requires opening the fracture. With external fracture fixation, the bone fragments are held in alignment by pins placed through the skin onto the skeleton, structurally supported by external

bars. With internal fracture fixation, the bone fragments are held by wires, screws, plates, and/or intramedullary devices [64].

Surgical wires are used to reattach large fragments of bone. They are also used to provide additional stability in long-oblique or spiral fractures of long bones which have already been stabilized by other means. Straight wires are called Steinmann pins. In the case of a pin diameter less than 2.38 mm, they are named Kirschner wires. They are widely used primarily to hold fragments of bones together provisionally or permanently and to guide large screws during insertion. *Screws* are the most widely used devices for fixation of bone fragments, Fig. 15.16a. There are two types of bone screws cortical bone screws, which have small threads, and cancellous screws, which have large threads to get more thread-to-bone contact. They may have either V or buttress threads. According to their ability to penetrate the cortical screws are subclassified further, into self-tapping and nonself-tapping. The self-tapping screws have cutting flutes that thread the pilot drill-hole during insertion. In contrast, the nonself-tapping screws require a tapped pilot drill-hole for insertion. The bone immediately adjacent to the screw often undergoes necrosis initially, but if the screw is firmly fixed when the bone revascularizes, permanent secure fixation may be achieved [65]. This is particularly true for titanium alloy screws or screws with a roughened thread surface, with which bone growth results in an increase in removal torque [65]. *Plates* are available in a wide variety of shapes and are intended to facilitate fixation of bone fragments, Fig. 15.16b. They range from the very rigid, intended to produce primary bone healing, to the relatively flexible, intended to facilitate physiological loading of bone. The rigidity and strength of a plate in bending depends on the cross-sectional thickness and material properties of which it is made. Consequently, the weakest region in the plate is the screw hole, especially if the screw hole is left empty, due to a reduction of the cross-sectional area in this region. The effect of the material on the rigidity of the plate is defined by the elastic modulus of the material for bending, and by the shear modulus for twisting [66]. Thus, given the same
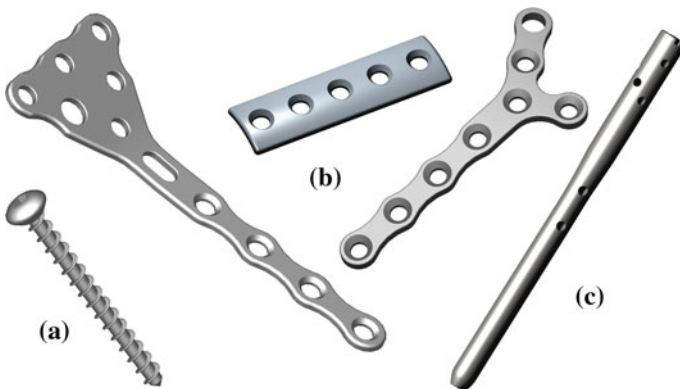

Fig. 15.16 Titanium trauma medical implants

dimensions, a titanium alloy plate will be less rigid than a stainless steel plate, since the elastic modulus of each alloy is 110 and 200 GPa, respectively. *Intramedullary devices (IM nails or rods)* are used as internal struts to stabilize long bone fractures, Fig. 15.16c. IM nails are also used for fixation of femoral neck or intertrochanteric bone fractures; however, this application requires the addition of long screws. A whole range of designs are available, going from solid to cylindrical, with shapes such as cloverleaf, diamond, and slotted cylinders. Compared to plates, IM nails are better positioned to resist multidirectional bending than a plate or an external fixator, since they are located in the center of the bone. However, their torsional resistance is less than that of the plate [66].

   The design of an implant for joint replacement should be based on the kinematics and dynamic load transfer characteristic of the joint. The material properties, shape, and methods used for fixation of the implant to the patient determines the load transfer characteristics. This is one of the most important elements that determines long-term survival of the implant, since bone responds to changes in load transfer with a remodeling process, known as Wolff's law. Overloading the implant-bone interface or shielding it from load transfer may result in bone resorption and subsequent loosening of the implant [67]. *The endoprosthesis for total hip replacement* consists of a femoral component and an acetabular component, Fig. 15.16b. The femoral stem is divided into head, neck, and shaft. The femoral stem is made of Ti alloy or Co–Cr alloy and is fixed into a reamed medullary canal by cementation or press fitting. The femoral head is made of Co–Cr alloy, aluminum, or zirconium. Although Ti alloy heads function well under clean articulating conditions, they have fallen into disuse because of their low wear resistance to third bodies, e.g., bone or cement particles. The acetabular component is generally made of ultra-high molecular weight polyethylene (UHMWPE). *The prosthesis for total knee joint replacement* consists of femoral, tibial, and/or patellar components, Fig. 15.17a. Compared to the hip joint, the knee joint has a more complicated geometry and movement mechanics, and it is not intrinsically stable.
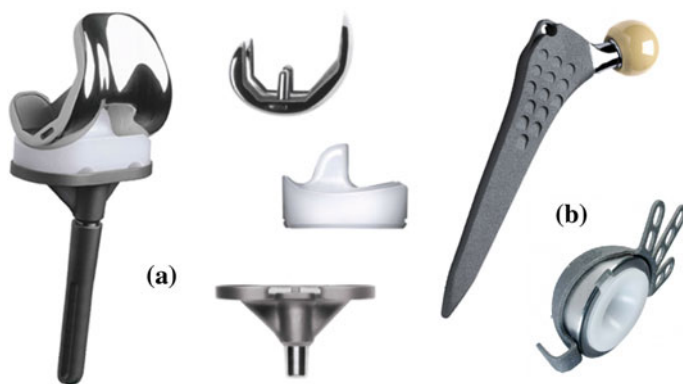

Fig. 15.17 Titanium orthopedics medical devices [130]

In a normal knee, the center of movement is controlled by the geometry of the ligaments. As the knee moves, the ligaments rotate on their bony attachments and the center of movement also moves. The eccentric movement of the knee helps distribute the load throughout the entire joint surface [68]. Total knee replacements can be implanted with or without cement, the latter relying on porous coating for fixation. The femoral components are typically made of Co–Cr alloy and the monolithic tibial components are made of UHMWPE. In modular components, the tibial polyethylene component assembles onto a titanium alloy tibial tray. The patellar component is made of UHMWPE, and a titanium alloy back is added to components designed for uncemented use.

For maxillofacial osteosynthesis in *the cranio-facial and mandibular areas titanium plate and screw systems* are preferred. In order to make them pliable, many of the plates are made from CP titanium sheet that is in the soft-recrystallized condition. The corresponding screws are either made from CP titanium or alloy and can be as small as 1 mm in diameter [69].

15.3 Shape Memory Alloys

15.3.1 Introduction

Smart materials have been given a lot of attention mainly for their innovative use in practical applications. One example of such materials is also the family of shape memory alloys (SMA) which are arguably the first well known and used smart material. Shape memory alloys possess a unique property according to which, after being deformed at one temperature, they can recover to their original shape upon being heated to a higher temperature. The effect was first discussed in the 1930s by Ölander [70] and Greninger and Mooradian [71]. The basic phenomenon of the shape memory effect was widely reported a decade later by Russian metallurgist G. Kurdjumov and also by Chang and Read [72]. However, presentation of this property to the wider public came only after the development of the nickel–titanium alloy (nitinol) by Buehler and Wang [73]. Since then, research activity in this field has been intense, and a number of alloys have been investigated, including Ag–Cd, Au–Cd, Cu–Zn, Cu–Zn–Al, Cu–Al–Ni, Cu–Sn, Cu–Au–Zn, Ni–Al, Ti–Ni, Ti–Ni–Cu, Ni–Ti–Nb, Ti–Pd–Ni, In–Ti, In–Cd and others. Crystallography of shape memory alloys have been studied for the past four decades. Only a fraction of the available literature is listed here [74–83]. Because these materials are relatively new, some of the engineering aspects of the material are still not well understood. Many of the typical engineering descriptors, such as Young's modulus and yield strength, do not apply to shape memory alloys since they are very strongly temperature dependent. On the other hand, a new set of descriptors must be introduced, such as stress rate and amnesia. That is why numerous constitutive models have been proposed over the past 25 years to predict thermomechanical behavior [84–97].

15.3.1.1 Thermomechanical Behavior

These materials have been shown to exhibit extremely large, recoverable strains (on the order of 10 %), and it is these properties as functions of temperature and stress that allow SMAs to be utilized in many exciting and innovative applications. From a macroscopic point of view, the mechanical behavior of SMAs can be separated into two categories: the *shape memory effect* (SME), where large residual (apparently plastic) strain can be fully recovered upon raising the temperature after loading and unloading cycle; and the *pseudoelasticity* or *superelasticity*, where a very large (apparently plastic) strain is fully recovered after loading and unloading at constant temperature. Both effects are results of a martensite phase transformation. In a stress-free state, an SMA material at high temperatures exists in the parent phase (usually a body-centered cubic crystal structure, also referred as the austenite phase). Upon decreasing the material temperature, the crystal structure undergoes a self-accommodating crystal transformation into martensite phase (usually a face-centered cubic structure). The phase change in the unstressed formation of martensite from austenite is referred to as 'self-accommodating' due to the formation of multiple martensitic variants and twins that prohibits the incurrence of a transformation strain. The martensite variants, evenly distributed throughout material, are all crystallographically equivalent, differing only by habit plane. The process of self-accomodation by twinning allows an SMA material to exhibit large reversible strains with stress. However, the process of self-accomodation in ordinary materials like stainless steel does not take place by twinning but via a mechanism called slip. Since slip is a permanent or unreversible process, the shape memory effect cannot occur in these materials. The difference between the twinning and slip process is shown in Fig. 15.18.

In the stress-free state, an SMA material has four transition temperatures, designated as M_f, M_S, A_S, A_f, i.e., Martensite Finish, Martensite Start, Austenite Start, and Austenite Finish, respectively. In the case of 'Type I' materials, temperatures are arranged in the following manner: $M_f < M_S < A_S < A_f$. A change of temperature within the range $M_S < T < A_S$ induces no phase changes and both phases can coexist within $M_f < T < A_f$. With these four transformation temperatures and the concepts of self-accommodation, the shape memory effect can be adequately explained. As an example let us consider a martensite formed from the parent phase
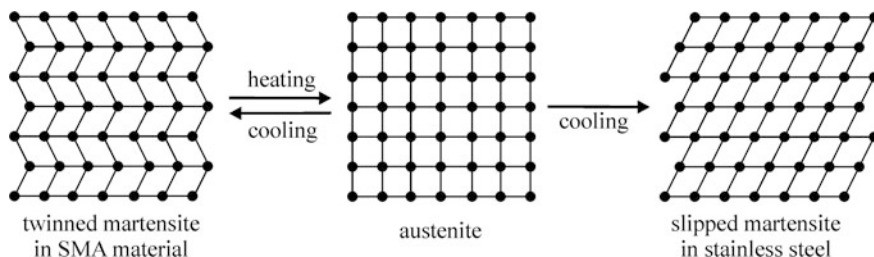

twinned martensite in SMA material   austenite   slipped martensite in stainless steel

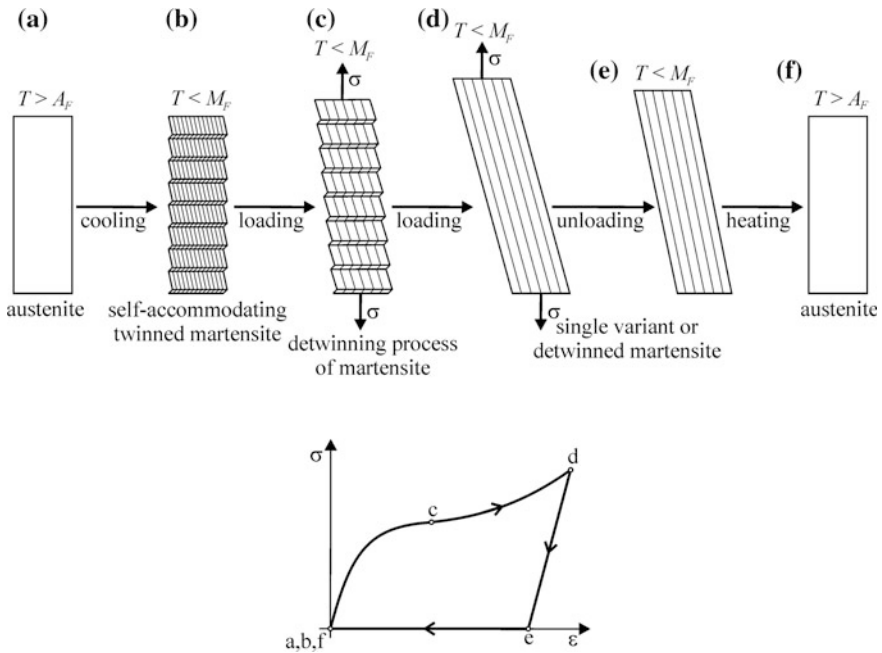**Fig. 15.18** Martensite transformation in shape memory alloys and steels

Fig. 15.19 Shape memory effect

(Fig. 15.19a) cooled under stress-free conditions through M_S and M_f. This material has multiple variants and twins present (Fig. 15.19b), all crystallographically equivalent but with different orientation (different habit plane indices). When a load applied to this material reaches a certain critical stress, the pairs of martensite twins begin 'de-twinning' to the stress-preferred twins (Fig. 15.19c). It means that the multiple martensite variants begin to convert to a single variant determined by alignment of the habit planes with the direction of loading (Fig. 15.19d). During this process of reorientation, the stress rises very slightly in comparison to the strain. As the single variant of martensite is thermodynamically stable at $T < A_S$, upon unloading there is no conversion to multiple variants and only a small elastic strain is recovered, leaving the material with a large residual strain (Fig. 15.19e). The de-twinned martensite material can recover the entire residual strain by simply heating above A_f; the material then transforms to the parent phase, which has no variants, and recovers to its original size and shape (Fig. 15.19f), thus creating the shape memory effect.

The pseudoelastic effect can be explained, if an SMA material is considered to be entirely in the parent phase (with $T > A_f$), Fig. 15.20a. When stress is applied to this material, there is a critical stress at which the crystal phase transformation from austenite to martensite can be induced, Fig. 15.20b. Due to the presence of stress during the transformation, specific martensite variants will be formed preferentially and at the end of transformation, the stress-induced martensite will consist of a
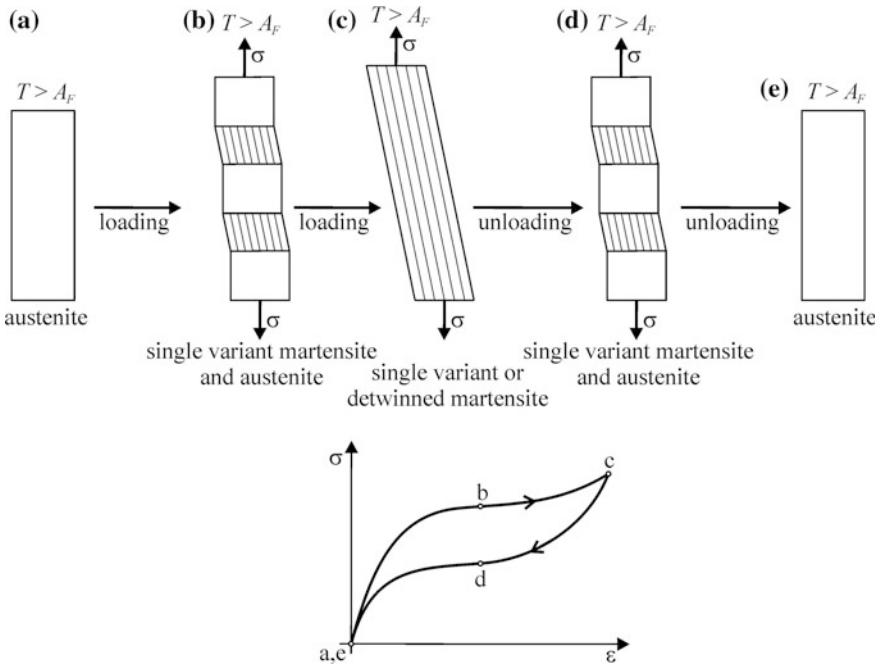
Fig. 15.20   Pseudoelasticity or superelasticity

single variant of detwinned martensite, Fig. 15.20c. During unloading, a reverse transformation to austenite occurs because of the instability of martensite at $T > A_f$ in the absence of stress, Fig. 15.20e. This recovery of high strain values upon unloading yields a characteristic hysteresis loop, diagram in Fig. 15.20, which is known as pseudoelasticity or superelasticity.

Many of the possible medical applications of SMA materials in the 1980s were attempting to use the thermally activated memory effect. However, temperature regions tolerated by the human body are very limited. Small compositional changes around the 50–50 % of Ti–Ni ratio can make dramatic changes in the operating characteristics of the alloy. Therefore, very precise control of phase transition temperatures is required. On the other hand, pseudoelasticity is ideally suited to medical applications since the temperature region of optimum effect can easily be located to encompass ambient temperature through body temperature.
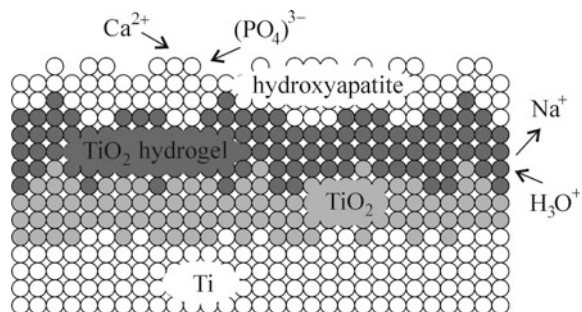
15.3.2   Biocompatibility

It is important to understand the direct effects of an individual component of the alloy since it can dissolve in the body due to corrosion and it may cause local and systemic toxicity, carcinogenic effects, and immune response. The cytotoxicity of

elementary nickel and titanium has been widely researched, especially in the case of nickel, which is a toxic agent and allergen [98–100]. Nickel is known to have toxic effects on soft tissue structures at high concentrations and also appears to be harmful to bone structures, but substantially less than cobalt or vanadium, which are also routinely used in implant alloys. Experiments with toxic metal salts in cell cultures have shown decreasing toxicity in the following order: $Co > V > Ni > Cr > Ti > Fe$ [101]. The dietary exposure to nickel is 160–600 mg/day. Fortunately most of it is eliminated in the feces, urine, and sweat. Pure nickel implanted intramuscularly or inside bone has been found to cause severe local tissue irritation and necrosis and high carcinogenic and toxic potencies. Due to corrosion of medical implants, a small amount of these metal ions is also released into distant organs. Toxic poisoning is later caused by the accumulation, processing and subsequent reaction of the host to the corrosion of the Ni-containing implant. Nickel is also one of the structural components of the metalloproteins and can enter the cell via various mechanisms. Most common Ni^{2+} ions can enter the cell utilizing the divalent cation receptor or via the support with Mg^{2+}, which are both present in the plasma membrane. Nickel particles in cells can be phagocytosed, which is enhanced by their crystalline nature, negative surface energy, appropriate particle size (2–4 μm), and low solubility. Other nickel compounds formed in the body are most likely to be NiCl and NiO, and fortunately there is only a small chance that the most toxic and carcinogenic compounds like Ni_3S_2, are to be formed. Nickel in soluble form, such as Ni^{2+} ions, enters through receptors or ion channels and binds to cytoplasmic proteins and does not accumulate in the cell nucleus at concentrations high enough to cause genetic consequences. These soluble Ni^{2+} ions and are rapidly cleaned from the body. However, the insoluble nickel particles containing phagocytotic vesicles fuse with lysosomes, followed by a decrease of phagocytic intravesicular pH, which releases Ni^{2+} ions from nickel containing carrier molecules. The formation of oxygen radicals, DNA damage, and thereby inactivation of tumor suppressor genes is contributed by that.

On the other hand, titanium is recognized to be one of the most biocompatible materials due to the ability to form a stable titanium oxide layer on its surface. In an optimal situation, it is capable of excellent osteointegration with the bone and it is able to form a calcium phosphate-rich layer on its surface, Fig. 15.21, very similar

Fig. 15.21 Formation of hydroxyapatite layer on titanium oxide film [131]

to hidroxyapatite which also prevents corrosion. Another advantageous property is that in case of damaging the protective layer the titanium oxides and Ca-P layer regenerate.

The properties and biocompatibility of nitinol have their own characteristics which are different from those of nickel or titanium alone. In vitro NiTi biocompatibility studies on the effects of cellular tolerance and its cytotoxicity have been performed on various cell culture models [102, 103]. Human monocytes and microvascular endothelial cells were exposed to pure nickel, pure titanium, stainless steel, and nitinol. Nitinol has been shown to release higher concentrations of Ni^{2+} ions in human fibroblast and osteoblast cultures, which did not affect cell growth [104–106]. Metal ion release study also revealed very low concentrations of nickel and titanium that were released from nitinol. Researchers therefore concluded that nitinol is not genotoxic.

For in vivo biocompatibility studies of nitinol effect, different experiments have been done on animals. Several in vivo nitinol biocompatibility studies that were done in the past decade disclosed no allergic reactions, no traces of alloy constituents in the surrounding tissue and no corrosion of implants. Studies of rat tibiae response to NiTi, compared with Ti-6Al-4V and stainless steel, showed that the number and area of bone contacts was low around NiTi implants, but the thickness of contact was equal to that of other implants. Normal new bone formation was seen in rats after 26 weeks after implantation. Good biocompatibility results of NiTi are attributed to the fact that implants are covered by a titanium oxide layer, where only small traces of nickel are being exposed.

15.3.2.1   Corrosion Behavior

The body is a complicated electrochemical system that constitutes an aggressive corrosion environment for implants which are surrounded by bodily fluids of an aerated solution containing 0.9 % NaCl, with minor amounts of other salts and organic compounds, serum ions, proteins, and cells which all may modify the local corrosion effect. High acidity of certain bodily fluids is especially hostile for metallic implants. Acidity can increase locally in the area adjacent to an implant due to inflammatory response of surrounding tissues mediating hydrogen peroxide and reactive oxygen and nitrogen compounds. The local pH changes for infected tissues or near haematoma are relatively small, however, these changes can alter biological processes and thereby the chemistry around the implant. It is known that small point corrosion or pitting prevails on surfaces of metallic implants. Another important feature is roughness of the surface which increases the reacting area of the implant and thereby adds to total amount of corrosion. Therefore, surface finishing is a major factor in improving corrosion resistance and consequently biocompatibility of medical devices [107, 108].

Corrosion resistance of SMA has also been studied in vivo on animals. Plates and stents have been implanted in dogs and sheeps for several months. Corrosion has been examined under microscope and pitting was established as predominant

after the implants were removed. Thus surface treatments and coatings were introduced. The improvement of corrosion resistance was considerable, since pitting decreased in some cases from 100 μm to only 10 μm in diameter.

15.3.3   Surface of Implant

The human response to implanted materials is a property closely related to the implant surface conditions. The major problems associated with the implants currently used are inadequate implant-tissue interface properties. Parameters that characterize surface property are chemical composition, crystallinity and heterogeneity, roughness and wettability or surface free energy that is a parameter important for cell adhesion. Each parameter is of great importance to biological response of the tissue. Another problem is implant sterilization that can remarkably modify desired parameters. Steam and dry sterilization are nowadays replaced by more advanced techniques such as hydrogen peroxide plasma, ethylene oxide, and electron and γ-ray irradiation.

The surface of NiTi SMA has revealed a tendency towards preferential oxidation of titanium. This behavior is in agreement with the fact that the free enthalpy of formation of titanium oxides is negative and exceeds in absolute value the enthalpy of formation of nickel oxides by at least two to three times. The result of oxidation is an oxide layer of a thickness between 2 and 20 nm, which consists mainly of titanium oxides TiO_2, smaller amounts of elemental nickel Ni^{2+}, and low concentrations of nickel oxides NiO. The surface chemistry and the amount of Ni may vary over a wide range, depending on the preparation method. The ratio of Ti/Ni on polished surface is around 5.5, while boiled or autoclaved items in water show decreased concentration of Ni on the surface and the Ti/Ni ratio increases up to 23–33 [109]. Different in vitro studies have shown how the physical, chemical and biocompatible properties of the implant surface can be improved [110–114].

15.3.3.1   Surface Improvements

Some of the most important techniques for improving the properties of Ni–Ti alloy surfaces are: (1) *Surface modification using energy sources and chemical vapors* such as hydroxyapatite, laser and plasma treatment, ion implantation, TiN and TiCN chemical vapor deposits. Hydroxyapatite coatings result in the best known biocompatibility and reveal a tendency to dissolution due to its relative miscibility with body fluids. Ion implantation and laser treatments usually result in surface amorphization that improves corrosion resistance, but the obtained amorphous surface layers are often not uniform. Laser surface melting leads to an increased oxide layer, decrease of Ni dissolution and improvement of the cytocompatibility up to classical Ti level. There is also a possibility that laser melted surfaces may be enriched in nickel, and become harder than bulk and swell. TiN and TiCN coatings are known to improve corrosion

resistance but large deformations caused by the shape memory effect may cause cracking of the coating. Therefore, for plates and staples a plasma-polymerized tetrafluoroethylene has been introduced; (2) *Development of bioactive surfaces* is another approach to improve biocompatibility of the SMA. Human plasma fibronectin covalently immobilized to NiTi surface improved the attachment of cells while corrosion rates were reduced drastically. Studies showed NiTi surface improved with this method caused a development of Ca-P layers, which in fact eliminate the need for hydroxyapatite coatings [111, 115]; (3) *Electrochemical processing for oxidation in air/oxygen* is a most common way of metal surface treatment. The technique combines electrochemical processes and oxidation in various media. Growth of native passive films that are highly adhesive and do not crack or break due to dynamic properties of SMA is promoted with this method. Oxide films obtained in air have different colors, thickness, and adhesive properties, with TiO_2 as a predominant oxide type; (4) *Oxidation of SMA medical devices in water and steam* is also one of the surface improvement techniques. Implants are preliminary chemically etched and boiled in water. The result is a surface with a very low Ni concentration, while etching removes surface material that was exposed to processing procedures and acquired various surface defects and heterogeneity. It also selectively removes nickel and oxidizes titanium. Surfaces obtained after oxidation in steam show better properties than those oxidized in water; and (5) *Electrochemical techniques* are commonly used to passivate NiTi surfaces. Surface passivation using electropolishing is often considered as a treatment of first choice just because this technique is used for surface conditioning of stainless steel, Co–Cr alloys, etc. However, the universal techniques developed for surface passivation of various alloys used for medical purposes are not necessary efficient for NiTi.

It should also be noted that the implant surface coatings are not always beneficial. The major problem of titanium-based alloys is that the formation of TiO_2, according to the chemical equation $Ti + 2H_2O \rightarrow TiO_2 + 4H^+ + 4e^-$, reduces the pH level at the titanium/coating interface. This means that if the coating is composed of hydroxyapatite, it can dissolve, which gradually leads to detachment of the coating.

15.3.4 Medical Applications

The trends in modern medicine are to use less invasive surgery methods that are performed through small, leak tight portals into the body called trocars. Medical devices made from SMAs use a different physical approach and can pull together, dilate, constrict, push apart and have made difficult or problematic tasks in surgery quite feasible. Therefore unique properties of SMAs are utilized in a wide range of medical applications. Some of the devices used in various medical applications are listed below.

Stents are most rapidly growing cardiovascular SMA cylindrical mesh tubes that are inserted into blood vessels to maintain the inner diameter of a blood vessel. The

product has been developed in response to limitations of balloon angioplasty, which resulted in repeated blockages of the vessel in the same area. Ni–Ti alloys have also become the material of choice for superelastic *self-expanding* (*SE*) *stents* that are used for a treatment of the superficial femoral artery disease (Fig. 15.22a). The SE nitinol stents are produced in the open state mainly with laser cut tubing and later compressed and inserted into the catheter. They can also be produced from wire and laser welded or coiled striped etched sheet. Before the compression stage, the surface of the stent is electrochemically polished and passivated to prescribed quality. Deployment of the SE stent is made with the catheter. During the operation procedure, when the catheter is in the correct position in the vessel, the SE stent is pushed out and then it expands against the inner diameter of the vessel due to a rise in temperature (thermally triggered device). This opens the iliac artery to aid in the normal flow of blood. The delivery catheter is then removed, leaving the stent within the patient's artery. Recent research has shown that implantation of a self-expanding stent provides better outcomes, for the time being, than balloon angioplasty [116–118]. *The Simon Inferior Vena Cava* (*IVC*) *filter* was the first SMA cardiovascular device. It is used for blood vessel interruption for preventing pulmonary embolism via placement in the vena cava. The Simon filter is filtering clots that travel inside bloodstream [119]. The device is made of SMA wire curved similarly to an umbrella that traps the clots that are better dissolved in time by the bloodstream. For insertion, the device is exploiting the shape memory effect, i.e., the original form in the martensitic state is deformed and mounted into a catheter. When the device is released, the body's heat causes the filter to return to its predetermined shape. *The Septal Occlusion System* is indicated for use in patients with complex ventricular septal defects (VSD) of significant size to warrant closures that are considered to be at high risk for standard transatrial or transarterial surgical closure based on anatomical conditions and/or based on overall medical condition. The system consists of two primary components; a permanent implant, which is constructed of an SMA wire framework to which polyester fabric is attached, and a coaxial polyurethane catheter designed specifically to facilitate attachment, loading, delivery and deployment to the defect [120]. The implant is placed by advancing the delivery catheter through blood vessels to the site of the defect inside the heart. The implant remains in the heart and the delivery catheter is removed. Instruments for minimally invasive surgery used in endoscopic surgery could not be feasible without implementation of SMA materials. The most representative instruments such as *guidewires*, *dilatators* and *retrieval baskets* exploit good kink resistance of SMAs [121]. *Open-heart stabilizers* are instruments similar to a steerable joint endoscopic camera. In order to perform bypass operations on the open-heart stabilizers are used to prevent regional heart movements while performing surgery. Another employment of the unique properties of SMAs such as constant force and superelasticity in heart surgery is a *tissue spreader* used to spread fatty tissue of the heart (Fig. 15.22b).

In general, conventional orthopedic implants by far exceed any other SMA implant in weight or volume. They are used as fracture fixation devices, which may or may not be removed and as joint replacement devices. Bone and nitinol have similar
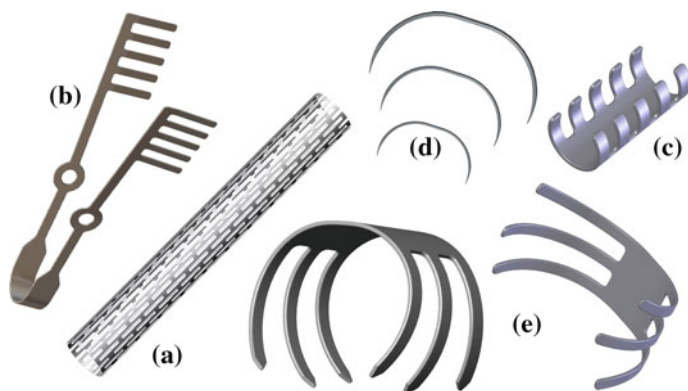
Fig. 15.22 Examples of nitinol medical devices

stress–strain characteristics, which makes nitinol a perfect material for production of bone fixation plates, nails, and other trauma implants [122]. In traditional trauma surgery bone plates and nails fixated with screws are used for fixation of broken bones. Shape memory fixators are one step forward applying a necessary constant force to faster fracture healing. *The SMA embracing fixator* consists of a body and sawtooth arms [123]. It embraces the bone about 2/3 of the circumference (Fig. 15.22c). The free ends of the arms that exceed the semi-circle are bent more medially to match the requirement fixation of a long tubular body whose cross section is not a regular circle. The applied axial compression stress is beneficial for enhancing healing and reducing segmental osteoporosis caused by a stress shielding effect. Its martensitic transformation temperature is 4–7 °C and shape recovery temperature is around the body's normal temperature, 37 °C. Similar to the embracing fixator is the so called *Swan-Like Memory-Compressive Connector* (*SMC*) for treatment of fracture and nonunion of upper limb diaphysis. The working principle of the device is similar with one important improvement. The SMC trauma implant is able to put constant axial stress to a fractured bone [124]. For fixation of tibial and femoral fractures nails fixated with screws are normally used. New *SMA inter-locking intramedullary nails* have many advantages compared to traditional ones. For example, when cooled SMA inter-locking nails are inserted into a cavity, guiding nails are extracted and body heat causes bending of nails into a preset shape applying constant pressure in the axial direction of the fractured bone [125]. The SMA effect is also used in surgical fixators made from wire. Certain devices that have been developed to fix vertebra in spine fractures are similar to an ordinary staple. *Staple shaped compression medical devices* are also used for internal bone fixation [126]. The compression staple is one of most simple and broadly used SMA devices in medicine (Fig. 15.22d). Since its introduction in 1981, over a thousand patients have been all successfully treated using this device. *The SMA Patellar Concentrator* was designed to treat patellar fractures (Fig. 15.22e). The device exerts continuous compression for the fixation of patella fracture. The shape of patellar concentrator consists of two basic patellae claws,
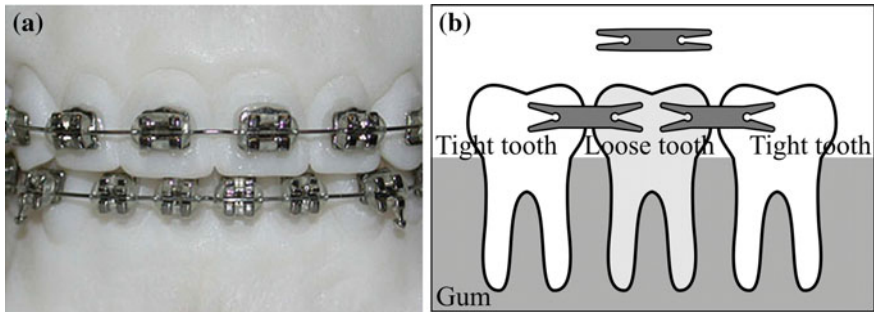
Fig. 15.23 Dental applications of nitinol

conjunctive waist, and three apex patellae claws. The thickness of the device may vary between 1.8 and 2.2 mm depending on different sizes of the concentrator. In clinical surgery, the claws are unfolded and put over fractured patella. Exposed to body temperature, the device tends to recover to its original state resulting in a recovery compressive force [127].

Dentists are using devices made from SMA for different purposes. NiTi-based SMA material performs exceptionally at high strains in strain-controlled environments, such as exemplified with *dental drills* for root canal procedures. The advantage of these drills is that they can be bent to rather large strains and still accommodate the high cyclic rotations [120]. Superelastic SMA wires have found wide use as orthodontic wires as well, Fig. 15.23a. *NiTi orthodontic archwire* was first produced in batches and clinically used in China in the beginning of 1980s [128]. Due to its unique property—superelasticity—the wire exerts gentle and retentive force to teeth, which is superior to stainless steel wire. Shape memory bracelets do not require as frequent visits to the dentist as the classical ones because of their ability to self adjust. The therapeutic period is therefore cut down by 50 %.

Lately a special *fixator for mounting bridgework* has been developed, Fig. 15.23b. A small piece of SMA metal is notch on both sides and placed between teeth and bridgework. As the temperature rises the notched area of metal is expanded on both sides causing a permanent hold of bridgework. The tooth fixator can also be used to prevent a loose tooth from falling out.

15.4 Conclusions

The use of titanium alloys as biomaterials has been growing due to their reduced elastic modulus, superior biocompatibility, high strength-to-weight ratio and enhanced corrosion resistance when compared to more conventional stainless steel and Co–Cr alloys. Ti-6Al-4V (and Ti-6Al-4V ELI), the most common titanium alloy is still the most extensively used titanium alloy for medical applications.

However, V and Al have been found to be toxic to the human body. In this context, β titanium alloys have been studied and developed and due to their high strength, biocompatible behavior, low elastic modulus, superior corrosion resistance, and good formability, they are likely to replace the classic α + β-type Ti-6Al-4V for medical applications in the near future.

SMA implants and medical devices have been successful because they offer a possibility of performing less invasive surgeries. Nitinol wires in medical instruments are more kink resistant and have smaller diameters compared to stainless steel 316L or polymer devices. Research to develop composite materials, containing SMA that will prove cost efficient and porous SMAs that will enable the transport of body fluids from the outside to inside of the bone is currently underway.

References

1. Sibum, H. (2003). Titanium and titanium alloys—from raw material to semi-finished products. *Advanced Engineering Materials, 5*(6), 393.
2. Wang, K. (1996). The use of titanium for medical applications in the USA. *Materials Science and Engineering A, 213*, 134.
3. Rack, H. J., & Qazi, J. I. (2006). Titanium alloys for biomedical applications. *Materials Science and Engineering C, 26*, 1269.
4. Niinomi, M. (2002). Recent metallic materials for biomedical applications. *Metallurgical and Materials Transactions, 33A*, 477.
5. Lütjering, G., & Williams, J. C. (2003). *Titanium*. Berlin: Springer-Verlag.
6. Long, M., & Rack, H. J. (1998). Titanium alloys in total joint replacement—a materials science perspective. *Biomaterials, 19*, 1621.
7. Katti, K. S. (2004). Biomaterials in total joint replacement. *Colloids and Surfaces B: Biointerfaces, 39*, 133.
8. Disegi, J. A. (2000). Titanium alloys for fracture fixation implants, Injury. *International Journal of the Care of the Injured, 31* (200) S-D14.
9. He, G., & Hagiwara, M. (2006). Ti alloy design strategy for biomedical applications. *Materials Science and Engineering C, 26*, 14.
10. Bannon, B. P., & Mild, E. E. (1983). Titanium alloys for biomaterial application: An overview, titanium alloys in surgical implants. In H. A. Luckey & F. Kubli, Jr (Eds.), *American Society for Testing and materials* (pp. 7–15). Pennsylvania: ASTM STP 796.
11. Oliveira, V., Chaves, R. R., Bertazzoli, R., & Caram, R. (1998). Preparation and characterization of Ti-Al-Nb orthopedic implants. *Brazilian Journal of Chemical Engineering, 17*, 326.
12. Boyer, R. R. (1996). Ana overview on the use of titanium in the aerospace industry. *Materials Science and Engineering A, 213*, 103.

13. Ferrero, J. G. (2005). Candidate materials for high-strength fastener applications in both the aerospace and automotive industries. *Journal of Materials Engineering and Performance, 14*, 691.

14. Semlitsch, M., Staub, F., & Weber, H. (1985). Titanium-aluminum-niobium alloy, development for biocompatible, high-strength surgical implants. *Biomedizinische Technik, 30*, 334.

15. Vail, T. P., Glisson, R. R., Koukoubis, T. D., & Guilak, F. (1998). The effect of hip stem material modulus on surface strain in human femora. *Journal of Biomechanics, 31*, 619.

16. Niinomi, M., Akahori, T., Takeuchi, T., Katsura, S., Fukui, H., & Toda, H. (2005). Mechanical properties and cyto-toxicity of new beta type titanium alloy with low melting points for dental applications. *Materials Science and Engineering C, 25*, 417.

17. Kikuchi, M., Takahashi, M., & Okuno, O. (2006). Elastic moduli of cast Ti-Au, Ti-Ag, and Ti-Cu alloys. *Dental Materials, 22*, 641.

18. Kim, H. S., Kim, W.-Y., & Lim, S.-H. (2006). Microstructure and elastic modulus of Ti-Nb-Si ternary alloys for biomedical applications. *Scripta Materialia*, *54*, 887–891.

19. Gross, S., & Abel, E. W. (2001). A finite element analysis of hollow stemmed hip prostheses as a means of reducing stress shielding of the femur. *Journal of Biomechanics, 34*, 995.

20. Hao, Y. L., Niinomi, M., Kuroda, D., Fukunaga, K., Zhou, Y. L., & Yang, R. (2003). Aging response of the Young's modulus and mechanical properties of Ti-29Nb-13Ta-4.6Zr. *Metallurgical and Materials Transactions, 34A*, 1007–1012.

21. Hao, Y. L., Niinomi, M., Kuroda, D., Fukunaga, K., Zhou, Y. L., Yang, R., et al. (2002). Young's modulus and mechanical properties of Ti-29Nb-13Ta-4.6Zr in relation to α″ martensite. *Metallurgical and Materials Transactions, 33A*, 3137–3144.

22. Gunawarman, B., Niinomi, M., Akahori, T., Souma, T., Ikeda, M., & Toda, H. (2005). Mechanical properties and microstructures of low cost β titanium alloys for healthcare applications. *Materials Science and Engineering C, 25*, 304.

23. Sakaguchi, N., Niinomi, M., Akahori, T., Takeda, J., & Toda, H. (2005). Relationship between tensile deformation behavior and microstructure in Ti-Nb-Ta-Zr. *Materials Science and Engineering C, 25*, 363.

24. Kuroda, D., Niinomi, M., Morinaga, M., Kato, Y., & Yashiro, T. (1998). Design and mechanical properties of new β type titanium alloys for implant materials. *Materials Science and Engineering A, 243*, 244.

25. Peters, M., Hemptenmacher, H., Kumpfert, J., & Leyens, C. (2003). In C. Leyens & M. Peters (Eds.), *Titanium and Titanium Alloys* (pp. 1–57). New York: Wiley-VCH.

26. Ari-Gur, P., & Semiatin, S. L. (1998). Evolution of microstructure, macrotexture and microtexture during hot rolling og Ti-6Al-4V. *Materials Science and Engineering A, 257*, 118.

27. Lütjering, G. (1999). Property optimization through microstructural control in titanium and aluminum alloys. *Materials Science and Engineering A, 263*, 117.

28. Prasad, Y. V. R. K., & Seshacharyulu, T. (1998). Processing maps for hot working of titanium alloys. *Materials Science and Engineering A, 243*, 82.

29. Freese, H. L., Volas, M. G., & Wood, J. R. in: D. M. Brunette, P. Tengvall, M. Textor & P. Thomsen (Eds.), *Titanium in medicine* (pp. 25–51). New York: Springer.

30. Froes, F. H., & Bomberger, H. B. (1985). The beta titanium alloys. *Journal of Metals, 37*, 28.

31. Karasevskaya, O. P., Ivasishin, O. M., Semiatin, S. L., & Matviychuk, Y. V. (2003). Deformation behavior of beta-titanium alloys. *Materials Science and Engineering A, 354*, 121.

32. Lin, D. J., Chern, J. H., & Ju, C. P. (2002). Effect of omega phase on deformation behavior of Ti-7.5Mo-xFe alloys. *Materials Chemistry and Physics, 76*, 191.

33. Moffat, D. L., & Larbalestier, D. C. (1988). The competition between the alpha and omega phases in aged Ti-Nb alloys. *Metallurgical Transactions, 19A*, 1687.

34. Flower, H. M., Henry, S. D., & West, D. R. F. (1974). The βα ⇆ αβ transformation in dilute Ti-Mo alloys. *Journal of Materials Science, 9*, 57.

35. Tang, X., Ahmed, T., & Rack, H. J. (2000). Phase transformations in Ti-Nb-Ta and Ti-Nb-Ta-Zr alloys. *Journal of Materials Science, 35*, 1805.
36. Dobromyslov, A. V., & Elkin, V. A. (2003). Martensitic transformation and metastable b-phase in binary titanium alloys with d-metals of 4–6 periods. *Materials Science and Engineering A, 354*, 121.
37. Dobromyslov, A. V., & Elkin, V. A. (2006). The orthorhombic α″-phase in binary titanium base alloys with d-metals of V–VIII groups. *Materials Science and Engineering A, 438*, 324–326 (in press).
38. Niinomi, M. (1998). Mechanical properties of biomedical titanium alloys. *Materials Science and Engineering A, 243*, 231.
39. Brunski, J. B. (2004). In B. D. Ratner, A. S. Hoffman, F. J. Schoen, & J. E. Lemons (Eds.), *Biomaterials science—an introduction to materials in medicine* (pp. 137–153). San Diego: Elsevier Academic Press.
40. Wataria, F., Yokoyamaa, A., Omorib, M., Hiraic, T., Kondoa, H., Uoa, M., & Kawasakia, T. (2004). Biocompatibility of materials and development to functionally graded implant for bio-medical application. *Composites Science and Technology, 64*, 893–908.
41. Black, J. (1992). *Biological performance of materials* (2nd ed.). New York: M. Dekker Inc.
42. Park, J. B., & Kim, J. B. (2000). Metallic biomaterials, chapter 37. In J. D. Bronzino & B. Raton (eds.), *The biomedical engineering handbook*, (2nd ed.). Boca Raton: CRC Press LLC.
43. Feighan, J. E., Goldberg, V. M., Davy, D., Parr, J. A., & Stevenson, S. (1995). The influence of surfaceblasting on the incorporation of titanium-alloy implants in a rabbit intramedullary model. *The Journal of Bone & Joint Surgery. American Volume, 77A*, 1380–1395.
44. Tengvall, P., & Lundstrom, I. (1992). Physico-chemical considerations of titanium as a biomaterial. *Clinical Materials, 9*, 115–134.
45. Henrich, V. E., & Cox, P. A. (1994). *The surface science of metal oxides*. Cambridge: Cambridge University Press.
46. Thull, R., & Grant, D. (2001). Physical and chemical vapor deposition and plasma-assisted techniques for coating titanium. In D. M. Brunette, P. Tengvall, M. Textor & P. Thomsen (Eds.), *Titanium in medicine* (pp. 284–335). Berlin Heidelberg: Springer-Verlang.
47. Klocke, F. (2001). *Manufacturing technology I*. Aachen: WZL-RWTH.
48. Jackson, M. J., & Morrell, J. S. (Eds.). (2015). *Machining with Nanomaterials* (2nd ed.). New York and Heidelberg: Springer.
49. Donachie, M. (2000). *Titanium—a technical guide* (2nd ed.). Materials Park, OH: ASM International.
50. Iqbal, S. A., Mativenga, P. T., & Sheikh, M. A. (2009). A comparative study of the tool-chip contact length in turning of two engineering alloys for a wide range of cutting speeds. *International Journal of Advanced Manufacturing Technology, 42*, 30–40.
51. Sun, J., & Guo, Y. B. (2008). A new multi view approach to characterize 3D chip morphology and properties in end milling titanium Ti6Al4V. *International Journal of Machine Tools and Manufacture, 48*, 1486–1494.
52. Cotterell, M., & Byrne, G. (2008). Dynamics of chip formation during orthogonal cutting of titanium alloy Ti-6Al-4V. *CIRP Annals - Manufacturing Technology, 57*, 93–96.
53. Barry, J., Byrne, G., & Lennon, D. (2000). Observations on chip formation and acoustic emission in machining. *International Journal of Machine Tools and Manufacture, 41*, 1055–1070.
54. Fang, N. (2003). Slip-line modeling of machining with a rounded-edge tool—Part II: Analysisof the size efect and the shear strain-rate. *Journal of the Mechanics and Physics of Solids, 51*, 43–762.
55. Komanduri, R. (1982). Some clarifications on the mechanics of chip formation when machining titanium alloys. *Wear, 76*, 15–34.
56. Abdelmoneim, M. E., & Scrutton, R. F. (1973). Post-machining plastic recovery and the law of abrasive wear. *Wear, 24*, 1–13.

57. Komanduri, R. (1971). Aspects of machining with negative rake tools simulating grinding. *International Journal of Design and Research MTDR, 11*, 223–233.

58. Rubenstein, C., Groszman, F. K., & Koenigsberger, F. (1967). *Force measurements during cutting tests with single point tools simulating action of single abrasive grit*. Paper presented at the International Industrial Diamond Conference.

59. Puerta Velasquez, J. D., Bolle, B., Chevrier, P., Geandier, G., & Tidu, A. (2007). Metallurgical study on chips obtained by high speed machining of a Ti-6 wt.%Al-4 wt.%V alloy. *Materials Science and Engineering A, 452–453*, 469–474.

60. Vyas, A., & Shaw, M. C. (1999). Mechanics of Saw-Tooth Chip Formation in Metal Cutting. *Journal of Manufacturing Science and Engineering, 121*, 163–172.

61. Morshed, M. M., McNamara, B. P., Cameron, D. C., & Hashmi, M. S. J. (2003). Stress and adhesion in DLC coatings on 316L stainless steel deposited by a neutral beam source. *Journal of Materials Processing Technology, 143*, 922–926.

62. Hench, L. L., Splittr, R. J., Allen, W. C., & Greenlec, T. K. (1971). Bonding mechanisms at the interface of ceramic prosthetic materials. *Journal of Biomedical Materials Research, 2*, 117–141.

63. de Groot, K., Klein, C. P. A. T., Wolke, J. G. C., & de Blieck-Hogervorst, J. M. A. (1990). *Plasma-sprayed coatings of calcium phosphate, CRC handbook of bioactive ceramics* (Vol. 2, pp. 133–142). Boston: CRC Press.

64. Hulth, A. (1989). Current concepts of fracture healing. *Clinical Orthopaedics and Related Research*, 249–265.

65. Hutzschenreuter, P., & Brümmer, H. (1980). Screw design and stability. In H. Uhthoff (Ed.), *Current concepts of Internal Fixation* (pp. 244–250). Berlin: Springer-Verlag.

66. Cochran, G. V. B. (1982). Biomechanics of orthopaedic structures. In *Primer in orthopaedic biomechanics* (pp. 143–215). New York: Churchill Livingstone.

67. Sarmiento, A., Ebramzadeh, E., & Gogan, W. J. (1990). Cup containment and orientation in cemented total hip arthroplasties. *Journal of Bone & Joint Surgery, 72B*(6), 996.

68. Burstein, A. H., & Wright, T. H. (1993). Biomechanics. In J. Insall, R Windsor & W. Scott (Eds.), *Surgery of the knee* (2nd ed., Vol. 7) (pp. 43–62). New York: Churchill Livingstone.

69. Perren, M. S., Pohler, O. E. M., & Schneider, E. (2001). Titanium as implant material for osteosynthesis applications. In D. M. Brunette, P. Tengvall, M. Textor & P. Thomsen (Eds.), *Titanium in medicine* (pp. 772–823). Berlin Heidelberg: Springer-Verlang.

70. Olander, A. (1932). An electrochemical investigation of solid cadmium-gold alloys. *Journal of the American Chemical Society, 54*, 3819–3833.

71. Greninger, A. B., & Mooradian, V. G. (1938). Strain transformation in metastable beta copper-zinc and beta copper-tin alloys. *AIME, 128*, 337–368.

72. Chang, L. C., & Read, T. A. (1951). Plastic deformation and diffusionless phase changes in metals-the gold-cadmium beta phase. *Transaction of the American Institute of Mining and Metallurgical Engineers, 191*(1), 47–52.

73. Buehler, W. J., & Wang, F. E. (1967). A summary of recent research on the Nitinol alloys and their potential application in ocean engineering. *Journal of Ocean Engineering, 1*, 105–108.

74. Wayman, C. M. (1964). *Introduction to the crystallography of martensitic transformations*. UK: The Macmillan Company.

75. Otsuka, K., & Wayman, C. M. (1998). *Shape memory materials*. Cambridge: Cambridge University Press.

76. Wechsler, M. S., Liberman, D. S., & Read, T. A. (1953). On the theory of the formation of martensite. *Transaction of the AIME, 197*, 1503–1515.

77. Bowles, J. S., & Mackenzie, J. K. (1954). The crystallography of martensite transformations I. *Acta Metallurgica, 2*, 129–137.

78. Saburi, T., & Wayman, C. M. (1979). Crystallographic similarities in shape memory martensites. *Acta Metallurgica, 27*(6), 979–995.

79. Adachi, K., Perkins, J., & Wayman, C. M. (1986). Type II twins in self-accommodating martensite plate variants in a Cu-Zn-Al shape memory alloy. *Acta Metallurgica, 34*(12), 2471–2485.
80. James, R. D., & Hane, K. F. (2000). Martensitic transformations and shape-memory materials. *Acta Materialia, 48*(1), 197–222.
81. Krishnan, Madangopal. (1998). The self accommodating martensitic microstructure of Ni-Ti shape memory alloys. *Acta Materialia, 46*(4), 1439–1457.
82. Inamura, T., Kinoshita, Y., Kim, J. I., Kim, H. Y., Hosoda, H., Wakashima, K., et al. (2006). Effect of {0 0 1} < 1 1 0 > texture on superelastic strain of Ti-Nb-Al biomedical shape memory alloys. *Materials Science and Engineering A, 438*, 865–869 (In Press).
83. Bhattacharya, K. (2003). *Microstructure of martensite: Why it forms and how it gives rise to the shape-memory effect, Oxford series on materials modelling* (1st ed.). Oxford: Oxford University Press.
84. Stalmans, R., Delaey, L., & Van Humbeeck, J. (1997). Generation of recovery stresses: Thermodynamic modelling and experimental verification. *Le Journal de Physique IV, 7*, 47–52.
85. Barsch, G. R., & Krumhansl, J. A. (1984). Twin boundaries in ferroelastic media without interface dislocations. *Physical Review Letters, 53*(11), 1069–1072.
86. Falk, F. (1980). Model free energy, mechanics, and thermodynamics of shape memory alloys. *Acta Metallurgica, 28*, 1773–1780.
87. Maugin, G. A., & Cadet, S. (1991). Existence of solitary waves in martensitic alloys. *International Journal of Engineering Science, 29*(2), 243–258.
88. Brinson, L. C., & Lammering, R. (1993). Finite element analysis of the behavior of shape memory alloys and their applications. *International Journal of Solids and Structures, 30*(23), 3261–3280.
89. Ivshin, Y., & Pence, T. J. (1993). A thermomechanical model for a one variant shape memory material. *Journal of Intelligent Material Systems and Structures, 5*(7), 455–473.
90. Liang, C., & Rogers, C. A. (1990). One-dimensional thermomechanical constitutive relations for shape memory materials. *Journal of Intelligent Material Systems and Structures, 1*(2), 207–234.
91. Boyd, J. G., & Lagoudas, D. C. (1994). Thermomechanical response of shape memory composites. *Journal of Intelligent Material Systems and Structures, 5*, 333–346.
92. Tanaka, K. (1986). A thermomechanical sketch of shape memory effect: One-dimensional tensile behavior. *Res Mechanica, 18*, 251–263.
93. Brinson, L. C. (1993). One-dimensional constitutive behavior of shape memory alloys: Thermomechanical derivation with non-constant material functions and redefined martensite internal variable. *Journal of Intelligent Material Systems and Structures, 4*, 229–242.
94. Lubliner, J., & Auricchio, F. (1996). Generalized plasticity and shape-memory alloys. *International Journal of Solids and Structures, 33*(7), 991–1003.
95. Panoskaltsis, V. P., Bahuguna, S., & Soldatos, D. (2004). On the thermomechanical modeling of shape memory alloys. *International Journal of Non-Linear Mechanics, 39*(5), 709–722.
96. Sun, Q. P., & Hwang, K. C. (1994). Micromechanics constitutive description of thermoelastic martensitic transformations. *Advances in Applied Mechanics, 31*, 249–298.
97. Kosel, F., & Videnic, T. (2007). Generalized plasticity and uniaxial constrained recovery in shape memory alloys. *Mechanics of Advanced Materials and Structures, 14*(1), 3–12.
98. Denkhaus, E., & Salnikow, K. (2002). Nickel essentiality, toxicity, and carcinogenicity. *Critical Reviews in Oncology/Hematology, 42*, 35–56.
99. Nieboer, E., Tom, R. T., & Sanford, W. E. (1988). Nickel metabolism in man and animals. In H. Sigel (Ed.), *Nickel and its role in biology: Metal ions in biological systems* (Vol. 23, pp. 91–121). New York: Marcel Dekker.
100. Fletcher, G. G., Rossetto, F. E., Turnbull, J. D., & Nieboer, E. (1994). Toxicity, uptake, and mutagenicity of particulate and soluble nickel compounds. *Environmental Health Perspectives*, *102*(Suppl 3), 69–79.

101. Yamamoto, A., Honma, R., & Sumita, M. (1998). Cytotoxicity evaluation of 43 metal salts using murine fibroblasts and osteoblastic cells. *Journal of Biomedical Materials Research, 39*, 331–340.

102. Shih, C., Lin, S., Chung, K., Chen, Y., Su, Y., Lai, S., et al. (2000). The cytotoxicity of corrosion products of Nitinol stent wires on cultured smooth muscle cells. *Journal of Biomedical Material Research, 52*, 395–403.

103. Wever, D. J., Veldhuizen, A. G., Sanders, M. M., Schakenraad, J. M., & Horn, J. R. (1997). Cytotoxic, allergic and genotoxic activity of a nickel-titanium alloy. *Biomaterials, 18*, 1115–1120.

104. Wataha, I. C., Lockwood, P. E., Marek, M., & Ghazi, M. (1999). Ability of Ni-containing biomedical alloys to activate monocytes and endothelial cells in vitro. *Journal of Biomedical Materials Research, 45*, 251–257.

105. Ryhänen, J., Niemi, E., Serlo, W., Niemelä, E., Sandvik, P., Pernu, H., et al. (1997). Biocompatibility of nickel-titanium shape memory metal and its corrosion behavior in human cell cultures. *Journal of Biomedical Materials Research, 35*, 451–457.

106. Wirth, C., Comte, V., Lagneau, C., Exbrayat, P., Lissac, M., Jaffrezic-Renault, N., et al. (2005). Nitinol surface roughness modulates in vitro cell response: A comparison between fibroblasts and osteoblasts. *Materials Science and Engineering C, 25*, 51–60.

107. Trepanier, C., Leung, T., Tabrizian, M., Yahia, L. H., Bienvenu, J., Tanguay, J., et al. (1999). Preliminary investigation of the effect of surface treatment on biological response to shape memory NiTi stents. *Journal of Biomedical Materials Research, 48*, 165–171.

108. Shabalovskaya, S. A. (2002). Surface, corrosion and biocompatibility aspects of Nitinol as an implant material. *Bio-Medical Materials and Engineering, 12*, 69–109.

109. Shabalovskaya, S. A. (1996). On the nature of the biocompatibility and on medical applications of NiTi shape memory and superelastic alloys. *BioMedical Materials and Engineering, 6*, 267–289.

110. Frauchiger, V. M., Schlottig, F., Gasser, B., & Textor, M. (2004). Anodic plasma-chemical treatment of CP titanium surfaces for biomedical applications. *Biomaterials, 25*, 593–606.

111. Lu, X., Zhao, Z., & Leng, Y. (2006). Biomimetic calcium phosphate coatings on nitric-acid-treated titanium surfaces. *Materials Science and Engineering: C, 27*(4), 700–708 (in Press).

112. Park, J., Kim, D. J., Kim, Y. K., Lee, K. H., Lee, K. H., Lee, H., et al. (2003). Improvement of the biocompatibility and mechanical properties of surgical tools with TiN coating by PACVD. *Thin Solid Films, 435*(1–2), 102–107.

113. Shevchenko, N., Pham, M. T., & Maitz, M. F. (2004). Studies of surface modified NiTi alloy. *Applied Surface Science, 235*, 126–131.

114. Endo, K. (1995). Chemical modification of metallic implant surfaces with biofunctional proteins (Part 1). Molecular structure and biological activity of a modified NiTi alloy surface. *Dental Materials Journal, 14*, 185–198.

115. Liu, F., Wang, F., Shimizu, T., Igarashi, K., & Zhao, L. (2006). Hydroxyapatite formation on oxide films containing Ca and P by hydrothermal treatment. *Ceramics International, 32*(5), 527–531.

116. Schillinger, M., Sabeti, S., & Loewe, C. (2006). Balloon angioplasty versus implantation of nitinol stents in the superficial femoral artery. *Journal of Vascular Surgery, 44*(3), 684.

117. Rapp, B. (2004). Nitinol for stents. *Materials Today, 7*(5), 13.

118. Tyagi, S., Singh, S., Mukhopadhyay, S., & Kaul, U. A. (2003). Self- and balloon-expandable stent implantation for severe native coarctation of aorta in adults. *American Heart Journal, 146*(5), 920–928.

119. Simon, M., Kaplow, R., Salzman, E., & Freiman, D. (1977). A vena cava filter using thermal shape memory alloy experimental aspects. *Radiology, 125*, 87–94.

120. Duerig, T., Pelton, A., & Stöckel, D. (1999). An overview of nitinol medical applications. *Materials Science and Engineering, A273–275*, 149–160.

121. Fischer, H., Vogel, B., Grünhagen, A., Brhel, K. P., & Kaiser, M. (2002). Applications of shape-memory alloys in medical instruments. *Materials Science Forum, V, 394–395*, 9–16.
122. Pelton, A. R., Stöckel, D., & Duerig, T. W. (2000). Medical uses of nitinol. *Materials Science Forum, 327–328*, 63–70.
123. Dai, K., Wu, X., & Zu, X. (2002). An investigation of the selective stress-shielding effect of shape-memory sawtooth-arm embracing fixator. *Materials Science Forum, 394–395*, 17–24.
124. Zhang, C., Xu, S., Wang, J., Yu, B., & Zhang, Q. (2002). Design and clinical applications of swan-like memory-compressive connector for upper-limb diaphysis. *Materials Science Forum, 394–395*, 33–36.
125. Da, G., Wang, T., Liu, Y., & Wang, C. (2002). Surgical treatment of tibial and femoral factures with TiNi Shape-memory alloy interlocking intramedullary nails. *Materials Science Forum, 394–395*, 37–40.
126. Song, C., Frank, T. G., Campbell, P. A., & Cuschieri, A. (2002). Thermal modelling of shape—memory alloy fixator for minimal-access surgery. *Materials Science Forum, 394–395*, 53–56.
127. Xu, S., Zhang, C., Li, S., Su, J., & Wang, J. (2002). Three-dimensional finite element analysis of nitinol patellar concentrator. *Materials Science Forum, 394–395*, 45–48.
128. Chu, Y., Dai, K., Zhu, M., & Mi, X. (2000). Medical application of NiTi shape memory alloy in China. *Materials Science Forum, 327–328*, 55–62.
129. Kokubo, T., Kim, H. M., & Kawashita, M. (2003). Novel bioactive materials with different mechanical properties. *Biomaterials, 24*(13), 2161–2175.
130. Lima-L to SpA, Medical Systems, Via Nazionale 52, 33030 Villanova di San Daniele del Friuli (Udine), Italy. http://www.lima.it/english/medical_syst.html
131. Combes, C., Rey, C., & Freche, M. (1998). XPS and IR study of dicalcium phosphate dihydrate nucleation on titanium surfaces. *Colloids and Surfaces B: Biointerfaces, 11*(1–2), 15–27.